Title

Retene, pyrene and phenanthrene cause distinct molecular-level changes in the cardiac tissue of rainbow trout (*Oncorhynchus mykiss*) larvae, Part 2 – Proteomics and metabolomics

Authors

Cyril Rigaud [a,*], Andreas Eriksson [a], Anne Rokka [b], Morten Skaugen [c], Jenna Lihavainen [d], Markku Keinänen [d], Heli Lehtivuori [e] and Eeva-Riikka Vehniäinen [a]

Affiliations

[a] Department of Biological and Environmental Sciences, University of Jyväskylä, Jyväskylä, Finland

[b] Turku Bioscience Centre, University of Turku and Åbo Akademi University, Turku, Finland

[c] Department of Chemistry, Biotechnology and Food Science, Norwegian University of Life Sciences, Ås, Norway

[d] Department of Environmental and Biological Sciences, Joensuu Campus, University of Eastern Finland, Joensuu, Finland

[e] Department of Physics, Nanoscience Center, University of Jyväskylä, Jyväskylä, Finland

* Address correspondence to cyril.c.rigaud@jyu.fi

Abstract

Polycyclic aromatic hydrocarbons (PAHs) are global contaminants of concern. Despite several decades of research, their mechanisms of toxicity are not very well understood. Early life stages of fish are particularly sensitive with the developing cardiac tissue being a main target of PAHs

toxicity. The mechanisms of cardiotoxicity of the three widespread model polycyclic aromatic hydrocarbons (PAHs) retene, pyrene and phenanthrene were explored in rainbow trout (*Oncorhynchus mykiss*) early life stages. Newly hatched larvae were exposed to sublethal doses of each individual PAH causing no detectable morphometric alterations. Changes in the cardiac proteome and metabolome were assessed after 7 or 14 days of exposure to each PAH. Phase I and II enzymes regulated by the aryl hydrocarbon receptor were significantly induced by all PAHs, with retene being the most potent compound. Retene significantly altered the level of several proteins involved in key cardiac functions such as muscle contraction, cellular tight junctions or calcium homeostasis. Those findings were quite consistent with previous reports regarding the effects of retene on the cardiac transcriptome. Significant changes in proteins linked to iron and heme metabolism were observed following exposure to pyrene. While phenanthrene also altered the levels of several proteins in the cardiac tissue, no clear mechanisms or pathways could be highlighted. Due to high variability between samples, very few significant changes were detected in the cardiac metabolome overall. Slight but significant changes were still observed for pyrene and phenanthrene, suggesting possible effects on several energetic or signaling pathways. This study shows that early exposure to different PAHs can alter the expression of key proteins involved in the cardiac function, which could potentially affect negatively the fitness of the larvae and later of the juvenile fish.

Keywords: aquatic toxicology**,** cardiotoxicity, developmental toxicity, metabolomics, polycyclic aromatic hydrocarbons (PAHs), proteomics

1. Introduction

Polycyclic aromatic hydrocarbons (PAHs) are among the most ubiquitous environmental contaminants of global concern (Rubailo and Oberenko, 2008). Originating from both pyrogenic

or petrogenic sources, their influx into to the environment is believed to have increased over the past decades because of increasing human activities (Kurek et al., 2013). PAHs usually end up in the aquatic environment following for example atmospheric deposition, human-related effluents (municipal or industrial), surface runoffs or natural and accidental oil spills (Wolska et al., 2012). Aquatic organisms are chronically exposed to PAHs by direct contact with the water column, the sediment or by preying on other potentially contaminated organisms (Logan, 2007). During accidental episodes (e.g. the 2010 *Deepwater Horizon* disaster) resulting in the release of large quantities of oil in a short period of time into the aquatic environment, fish communities can be exposed to concentrations of PAHs high enough to be threatening at the population level (Incardona et al., 2014; Incardona et al., 2015). PAHs are listed as priority substances for the aquatic environment under the EU Water Framework Directive (Water Framework Directive, 2000). In the US, the EPA has 16 PAHs classified as priority pollutants (Keith, 2015), an approach that has sometimes being judged outdated and inadequate (Andersson and Achten, 2015).

Some PAHs are able to bind with the aryl hydrocarbon receptor (AhR) and induce dioxin-like toxicity in early life stages (ELS) of fish (Billiard et al., 1999; Scott et al., 2011). Dioxin-like toxicity in ELS of fish is often associated with the induction of detoxification enzymes (e.g. cytochrome P4501A) and characterized by the so-called blue sac disease (BSD) syndrome, which was first described in salmonids exposed to the model compound 2,3,7,8-tetrachlorodibenzo-*p*-dioxin (TCDD). The BSD syndrome includes various symptoms such as delayed growth, skull and jaw deformities, cardiovascular defects, pericardial and yolk sac edemas, hemorrhages and potentially death. Most importantly, the cardiac tissue appears to be the primary target of dioxin-like compounds (DLCs), as cardiovascular defects are the first

symptoms observed in fish ELS exposed to DLCs (Doering et al., 2019). However, not all PAHs are able to bind efficiently with the AhR (Barron et al., 2004). Some PAHs described as weak AhR agonists are able to induce AhR-independent cardiotoxicity in ELS of fish, including symptoms such as pericardial edemas usually linked to DLCs (Incardona et al., 2005). Overall, and despite almost two decades of research, the mechanisms of toxicity of PAHs are still poorly understood.

Retene (7-isopropyl-1-methylphenantrene) is an alkylated three-ring PAH commonly found in pulp and paper mill effluents (Leppänen and Oikari, 2001), but also formed by thermal degradation of resin compounds during wood combustion (Shen et al., 2012). Retene was reported at concentrations in the $ng.L^{-1}$ range in the surface water and in the $ng.g^{-1}$ range in the sediment of North American lakes or rivers (Ahad et al., 2015; Geier et al., 2018; Ruge et al., 2015). In sediments historically contaminated by pulp and paper mill effluents, concentrations ranging from several hundreds and several thousands of $\mu g.g^{-1}$ can be found (Leppänen and Oikari, 2001; Meriläinen et al., 2006). Contaminants sequestrated in the sediment can be released and made bioavailable to fish when the sediment is disturbed (Eggleton and Thomas, 2004). Retene is a potent AhR agonist capable of inducing dioxin-like toxicity in ELS of fish, as well as significant changes in the cardiac transcriptome of rainbow trout (*Oncorhyncus mykiss*) larvae at sublethal doses (Billiard et al., 1999; Scott et al., 2011; Vehniäinen et al., 2016). Retene was also recently described as a potential mediator of the cardiac function by altering the action potential as well as the intensity of ionic currents in rainbow trout ventricular cardiomyocytes exposed *in vitro* (Vehniäinen et al., 2019). Pyrene is another widespread PAH known to be an AhR agonist able to induce ELS dioxin-like toxicity in fish, including alteration of the cardiac function (Barjhoux et al., 2014; Hendon et al., 2008; Shi et al., 2012; Zhang, Y. et al., 2012). Pyrene is a

weaker AhR agonist compared to retene (Barron et al., 2004). While the knockdown of *cyp1a* using morpholino oligonucleotides appeared inefficient to protect from the embryotoxic effects of retene in zebrafish (*Danio rerio*) (Scott et al., 2011), an opposite result was observed for pyrene in the same species (Incardona et al., 2005). This suggests distinct mechanisms of toxicity between retene and pyrene following AhR activation, or distinct non-AhR mediated pathways between these two PAHs.

Phenanthrene is a three-ring PAH, known to be among the most abundant PAH compound in the air, in precipitation and in coastal and estuarine waters and sediments (Latimer and Zheng, 2003). Pyrene and phenanthrene can reach concentrations in the $\mu g.L^{-1}$ range in surface water impacted by industrialized areas, and up to several hundreds of $\mu g.L^{-1}$ close to crude oil exploitation (Anyakora et al., 2005; Maskaoui et al., 2002). Phenanthrene is a good example of PAHs that have a very low affinity with the AhR (Barron et al., 2004) but are still able to produce cardiotoxicity in fish ELS. The cardiotoxic effects of phenanthrene have been described in several fish species and include defects in heart looping, pericardial edemas, changes in the cardiac rhythm (bradycardia and arrhythmias), atrioventricular conduction blockage and reduction of blood circulation (Cypher et al., 2017; Incardona et al., 2004; Incardona et al., 2005; Mu et al., 2014; Sun, L. et al., 2015; Zhang, Y., Huang, Zuo et al., 2013; Zhang, Y., Huang, Wang et al., 2013). One possible mechanism of cardiotoxicity of phenanthrene in fish involves the alteration of the action potential and key ionic currents, as demonstrated *in vitro* in cardiomyocytes of the rainbow trout, the Pacific bluefin tuna (*Thunnus orientalis*) and the Pacific mackerel (*Scomber japonicus*) (Brette et al., 2017; Vehniäinen et al., 2019).

The main objective of the present study was to investigate the mechanisms of cardiotoxicity of the PAHs retene, pyrene and phenanthrene during the early life stages of a model fish species,

the rainbow trout. OMICs methods such as transcriptomics, proteomics and metabolomics have gained popularity in ecotoxicological studies, as they allow to study hundreds of molecular signals at the same time (Gündel et al., 2012). The present work is part of a larger project in which several OMICs tools were combined in an attempt to better understand the mechanisms of cardiotoxicity of PAHs. The changes in the cardiac transcriptome, proteome and metabolome following exposure to those model PAHs were assessed using a similar experimental setup. This manuscript reports the proteomic and metabolomic data, while the transcriptomic data was published separately (submitted manuscript).

2. Materials and methods

2.1. Chemicals

Pyrene (>98% purity), phenanthrene (≥99.5% purity) and dimethyl sulfoxide (DMSO, anhydrous, ≥99.9% purity) were all purchased from Sigma-Aldrich (St-Louis, MO, USA). Retene (≥98% purity) was obtained from MP Biomedicals (Illkirch, France). Stock solutions of each individual PAH were prepared by dissolving them in DMSO to reach concentrations of 3.2 $mg.mL^{-1}$ for retene and pyrene, and 10 $mg.mL^{-1}$ for phenanthrene.

2.2. Experimental design

Exposure tanks (N = 52) consisted of 1.5L Pyrex glass bowls filled with 1L of filtered lake water (Lake Konnevesi, Konnevesi, Finland) and were prepared 24h before the start of the exposures. The dissolved organic carbon (DOC) in the filtered lake water ranged between 7,0 and 8,2 $mg.L^{-1}$ (unpublished results). The bowls were randomly split between four different treatments (N = 13 tanks per treatment): DMSO (0.001%), retene (RET, 32 $\mu g.L^{-1}$), pyrene (PYR, 32 $\mu g.L^{-1}$) and phenanthrene (PHE, 100 $\mu g.L^{-1}$). The quantity of DMSO per tank was the same in all tanks (10

µL of pure DMSO or of the appropriate PAH stock solution into 1L of lake water). These exposure concentrations were selected based on previous studies in the case of retene (Billiard et al., 1999), and from preliminary experiments (unpublished results) for pyrene and phenanthrene. The concentrations used in the present study were chosen to be sublethal and to cause cardiotoxic effects such as pericardial edemas and arrhythmias. Rainbow trout (*Oncorhynchus mykiss*) eyed embryos at 360 degree-days (°D) of development were obtained from a local fish farm (Hanka-Taimen, Hankasalmi, Finland). Healthy (i.e. with no visible deformity) and newly hatched (<24h) embryos were randomly distributed into twelve tanks per treatment (N = 15 embryos per bowl, 720 embryos in total). Four tanks (one per treatment) were left without fish, for PAH concentration measurements. The water in the exposure tanks was completely renewed daily and fresh chemicals were added to ensure constant exposure to PAHs (i.e. semi-static exposure). The water temperature was measured every day and pH, conductivity and dissolved oxygen were monitored on a regular basis. The light:dark cycle was set on 16h:8h, and yellow fluorescent tubes were used. Larval mortality was monitored daily.

The procedure described above was reproduced three times, for three separate experiments: the larvae were sampled after either 7 (one experiment) or 14 days (two experiments, but one with only 9 tanks per treatment, including one without fish) of exposure. During sampling, all larvae were scored for signs of BSD (pericardial and yolk sac edemas, hemorrhages, craniofacial and spinal deformities) and a severity index ranging from 0 to 1 was calculated for each tank according to Villalobos et al. (2000), with some minor modifications described in Scott and Hodson (2008). All individuals were quickly and cautiously dissected under a microscope. The heart of each larva was isolated from the rest of the body using fine forceps (Dumont #5, Fine Science Tools, Heidelberg, Germany). The hearts of the larvae from two or three different tanks

per treatment were pooled together, thus each treatment consisted of four samples containing 30 or 45 hearts each. The samples (N = 32) used for the proteomics assay described in the present study were the same samples as the ones used for the transcriptomics assay after 7 and 14 days of exposure (submitted manuscript). The samples (N = 16) used for the metabolomics assay described in the present study were from the second 14 days exposure described above. All samples (N= 4 per treatment and each time point, for both the proteomics and the metabolomics) were immediately frozen in liquid nitrogen and then stored at -80°C until further analyses.

2.3. Measurements of PAH concentration in water

Depending on the duration of the experiment (7 or 14 days), water samples were collected after 1, 3, 7, 10 and 14 days of exposure, before the daily renewal of the exposure water. Concentrations measured by SFS right after the daily renewal are very close to the nominal values (Honkanen et al., 2020; unpublished results). Sample collection was performed by pipetting 5 mL of exposure water from four randomly chosen tanks per treatment, as well as from each tank lacking fish at the beginning of the experiment (one per treatment). Before storage at 4°C, 5 mL of ethanol (99.5% purity) was added in each sample.

The measurements were performed by synchronous fluorescence spectroscopy (SFS) using a LS-55 Fluorescence Spectrometer (PerkinElmer, Waltham, MA, USA), following the method and parameters previously described (submitted manuscript). More details regarding the method are available in the Supplementary file 1. Retene and phenanthrene water samples from the metabolomics exposure were affected by storage issues. Consequently, the only original data presented in the present manuscript are the pyrene concentrations and fluorescence spectrums from the 14 days exposure linked to the metabolomics assay. The PAH concentration data in water and carcasses of the larvae for proteomics assay exposures has been already presented

(submitted manuscript). Detailed methods and results for both measurements are accessible in the Supplementary file 1.

2.4. Protein extraction and measurements

The samples (N = 4) used for the protein extraction were the same as the ones used for the RNA extraction in the 7 and 14 days exposures presented in a different manuscript (submitted manuscript). After using the TRI Reagent (Molecular Research Center, Cincinnati, OH, USA) to isolate the aqueous phase containing the RNA, ethyl alcohol (99.5% purity) was added to the remaining organic phase and interphase to pellet the DNA. DNA was discarded and proteins were precipitated using isopropanol. After a series of successive washes using 0.3M guanidine hydrochloride (in 95% ethyl alcohol) and ethyl alcohol (99.5% purity), protein resuspension was performed using a solution of 8M urea and 2M thiourea in a 1M Tris-HCl buffer (pH 8.0).

Before the in-solution trypsin digestion, 15 µg of protein for each sample were reduced with dithiothreitol (1h at 37°C) and alkylated by iodoacetamide (1h at room temperature). Urea was diluted below 1M using 50 mM Tris-HCl. Trypsin was added in ratio 1:30 (w/w) and the samples were digested for 16h at 37°C. Digested peptides were desalted with SepPak C18 96-well plate (Waters, Milford, MA, USA) according to the instructions of the manufacturer, evaporated to dryness with SpeedVac (Thermo Fisher Scientific) and dissolved in 0.1% formic acid before MS analysis. Peptide concentrations were determined with NanoDrop™ (Thermo Fisher Scientific) by measuring absorbance at 280 nm. Concentrations of all samples were adjusted to 100 $ng.\mu L^{-1}$.

The LC-ESI-MS/MS analyses were performed on a nanoflow HPLC system (Easy-nLC1200, Thermo Fisher Scientific) coupled to the Q Exactive HF mass spectrometer (Thermo Fisher

Scientific) equipped with a nano-electrospray ionization source. Peptides were first loaded on a trapping column and subsequently separated inline on a 15 cm C18 column (75 µm x 15 cm, ReproSil-Pur 5 µm 200 Å C18-AQ, Dr. Maisch HPLC GmbH, Ammerbuch-Entringen, Germany). The mobile phase consisted of water with 0.1% formic acid (solvent A) or acetonitrile/water (80:20 (v/v)) with 0.1% formic acid (solvent B). A linear 120 min two steps gradient was used to elute peptides (85 min from 5% to 28% B, followed by 35 min from 28% to 40% B and finally 5 min wash with 100% B). All samples were injected twice, as technical replicates.

2.5. Metabolite extraction and processing

Alanine-d4 was obtained from Isotec (Sigma-Aldrich company), benzoic acid-d5 and glycerol-d8 were from Campro (Berlin, Germany), salicylic acid-13C from Icon (Schlüchtern, Germany), and alkane standard (C7-C40) from Supelco (Sigma-Aldrich company). N-methyl-N-(trimethylsilyl) trifluoroacetamide with 1% of trimethylsilyl chlorosilane (MSTFA with 1% of TMCS) was purchased from Thermo Fisher Scientific (Waltham, MA, USA). All other chemicals were from Sigma-Aldrich.

Metabolites were analyzed from three to four samples from each treatment (N = 3-4). Metabolites were extracted in two steps. First, cold methanol with 0.1% of formic acid (300 µL) and internal standard solution (10 µL) (0.24 $mg.mL^{-1}$ of alanine-d_4, 0.9 $mg.mL^{-1}$ of benzoic acid-d_5, 0.25 $mg.mL^{-1}$ of glycerol-d_8, 0.08 $mg.mL^{-1}$ of salicylic acid-^{13}C, 0.38 $mg.mL^{-1}$ of 4-methylumbelliferone in 8:8:3 H_2O:MeOH:DMSO) were added to the samples. Samples were then homogenized with a bead mill (5 mm stainless steel beads, 2×15s, 20 Hz, Qiagen TissueLyser). The metabolites were extracted with an Eppendorf Thermomixer for 15 min at 4°C at 1400 rpm. After a short centrifugation (2 min, 10°C, 13500g), supernatant was transferred to a

new test tube. The second extraction step was performed with cold 80% aqueous methanol with 0.1% formic acid (300 µL). Samples were homogenized with a beadmill, and metabolites were extracted for 5 min at 4°C at 1400 rpm. Samples were shortly centrifuged and the two supernatants were combined. Aliquots (200 µL) were transferred to vials and dried in a vacuum at 35°C for 40 min. Quality control samples (QC) were prepared by combining extracts from each sample group and included in each GC-MS analysis batch. Vials were treated with nitrogen gas before they were capped and stored overnight at -70°C.

Samples were taken out of the freezer and allowed to reach room temperature before the vials were opened. Dichloromethane (50 µL) was added to each sample and dried in a vacuum for 5 min. Samples were derivatized with 50 µL of 20 $mg.mL^{-1}$ methoxyamine hydrocloride in pyridine (MAHC) at 37°C for 90 min under continuous shaking (150 rpm). Samples were silylated with 70 µL of MSTFA with 1% of TMSC at 37°C for 60 min under continuous shaking (150 rpm). Alkane series in hexane (5 µL; C7-C40) was added to each sample as a retention time standard. Hexane (100 µL) was added to each sample before GC-MS analysis. GC-MS analysis was performed with an Agilent 6890N chromatography system coupled with a 5973N mass spectrometer, and a 7683 autosampler and injector. The injector was operated with pulsed splitless mode (1 µL) with a 30 psi pulse for 0.60 min and purge flow at 0.50 min. Injection temperature was set to 260°C and the sample was injected in a deactivated gooseneck splitless liner with glass wool. Helium flow to the column (30 m Rxi-5Sil MS, 0.25 mm ID, 0.25 µm film thickness with 10 m Integra-Guard, Restek) was kept constant at 1 $mL.min^{-1}$ and purge flow was 46 $mL.min^{-1}$. MSD interface temperature was 280°C, MS source 230°C and quadrupole 150°C. The oven temperature program was as follows: at 60°C for 3 min, 7°C min^{-1} ramp to 240°C, 10°C min^{-1} ramp to 330°C, 2 min at 330°C and post-run at 60°C for 6 min. Mass spectra were

collected with a scan range of 55-550 *m/z* with 2.94 scans s^{-1} and for metabolite annotation QC sample was analyzed with a wider scan range of 55-700 *m/z*.

Deconvolution, component detection and quantification were performed with Metabolite Detector (versions 2.06 beta and 2.2N) (Hiller et al., 2009) and AMDIS (version 2.66, NIST). Metabolite content was calculated as the peak area of the metabolite normalized with the peak area of the internal standard, benzoic-d_5 acid, and the dry weight of the sample. Metabolites were annotated based on spectra and retention index matched to reference compounds, and databases: the Golm Metabolome database (GMD) (Hummel et al., 2007) and the NIST Mass Spectral database (version 2.2 Agilent Technologies).

2.6. Bioinformatics and statistical analyses

2.6.1. Proteomics and metabolomics

Raw LC-ESI-MS/MS files were processed through MaxQuant 1.6.2.3 (Cox and Mann, 2008) for protein identification and label-free quantification (LFQ). The search engine Andromeda (Cox et al., 2011), integrated to the MaxQuant environment, was used to search proteins against two RefSeq databases during two separate MaxQuant runs: one for *O. mykiss* and one for the Atlantic Salmon (*Salmo salar*). Trypsin/P was used as the digestion mode parameter, with a maximum of two missed cleavages allowed. Variable modifications were set on N-terminal acetylation, oxidation of methionine and deamidation of asparagines and glutamines. The "match between runs" parameter of MaxQuant was set on 0.7 min for the match time window and 20 min for the alignment time window.

Statistical analyses were performed using R 3.5.1 (The R Foundation for Statistical Computing) and Bioconductor 3.8, with the significant level set at $\alpha = 0.05$. The analyses of the MaxQuant

output were performed using the R package DEP 1.5.1 (Zhang, X. et al., 2018). This package was favorited over the traditionally used Perseus software in order to apply the LIMMA approach (Linear Models for Microarray Data) to our dataset. This approach has been proved more powerful than the ordinary *t*-tests when the number of samples or replicates is small (Kammers et al., 2015). Proteins detected with less than two peptides were removed from the dataset. The data was filtered for proteins which were not quantified in all replicates: only the proteins identified in at least 3 out of 4 replicates of at least one treatment were retained for the analyses. The data was background corrected and normalized using the variance stabilizing transformation. Intensity distributions for proteins with and without missing values were inspected to establish that the missing values were mostly related to low intensities values. Thus, missing values were imputed using the "MinProb" function of the MSnbase (Gatto and Lilley, 2011) Bioconductor package integrated into DEP 1.5.1. The data was expressed as $\log_2$ of the fold changes ($\log_2$-FC) compared to the control samples (DMSO). A protein was considered as significantly differentially expressed if the $\log_2$-FC $\geq|0.4|$ with the false discovery rate (FDR) for the adjusted *p*-values set to 5%. The *k*-means clustering and heat map for the differentially expressed proteins were produced using the DEP package with the default parameters (Euclidean distance). Proteins that were identified exclusively by using the *S. salar* RefSeq database are presented separately from those heatmaps. GO (Gene Ontology) terms obtained from the Uniprot and QuickGO databases were used to help identifying the functions of all differentially expressed proteins. As more GO annotations were available for *S. salar* than for *O. mykiss*, all *O. mykiss* proteins Uniprot IDs were converted to *S. salar* Uniprot IDs using the NCBI BLAST software 2.7.1 algorithm (National Center for Biotechnology Information, Bethesda, MD, USA).

Two differentially expressed proteins were labelled as "uncharacterized protein" in the *O. mykiss* and *S. salar* databases. Their RefSeq sequences were submitted to BLASTp for identification.

The R package DEP 1.5.1 was applied for the statistical analyses of the metabolomics data as well. A total of 69 annotated metabolites were included in the analysis. The data was expressed as $\log_2$ of the fold changes ($\log_2$-FC) compared to the control samples (DMSO). For all other data, the normal distribution was assessed with the Shapiro-Wilk test. For the mortality data, which was expressed as proportions (%) of individuals, differences among treatments were assessed using the Fisher's exact test (FE). For other data, differences among treatments were tested using a one-way ANOVA followed by multiple comparisons Tukey's HSD test for normally distributed data, and a non-parametric Kruskal-Wallis test (KW) followed by Conover's test in other cases. All analyses were performed using R 3.5.1 (The R Foundation for Statistical Computing).

2.6.2. Pathway enrichment analysis

Pathways enrichment analyses (PEAs) were performed using the web-based tool PaintOmics 3 (v0.4.5). PaintOmics allow users to perform PEA using multiple OMICs datasets (Hernández-de-Diego et al., 2018). The tool first evaluates for each dataset the subset of genes, proteins or metabolites that participate in a particular KEGG pathway (Kyoto Encyclopedia of Genes and Genomes, Kyoto University, Japan). It evaluates the fraction of those biological features which overlaps with the set of features that the researcher considered relevant, and finally computes the significance of the overlap using the Fisher's exact test. When several tests for different datasets are performed for a single pathway (e.g. for proteomics and metabolomics), a single *p*-value is computed using the Fisher's combined probability test.

PEAs were performed for each compound and each sampling point: only proteomics datasets were included for the analyses related to day 7, while the analyses related to day 14 included both the proteomics and metabolomics datasets. Proteins Uniprot IDs had to be converted to zebrafish (*Danio rerio*) Entrez Gene ID prior to the PEA, since this is the only fish species and gene/protein nomenclature supported by KEGG pathways. This was done by gathering each RefSeq nucleotide ID linked to each Uniprot ID for *S. salar* or *O. mykiss* on the Uniprot database and submitting those RefSeq nucleotide IDs to the NCBI BLAST software 2.7.1 algorithm. The BLAST output was filtered to keep only the matches with *E*-values $\leq 10^{-3}$. Matches with *E*-values superior to this threshold were checked manually.

The proteomics datasets were submitted to PaintOmics as two separate files for each compound and time point: one "data" file containing the list of all proteins and their corresponding $\log_2$-FC and one "relevant" file containing only the list of proteins that were found to be significantly differentially expressed for that particular compound and time point. Similar files were generated and submitted to PaintOmics for the metabolomics datasets. All metabolites with a $\log_2$-FC $\geq$ |0.4| were considered as "relevant" for the PEAs.

3. Results

3.1. Mortality and deformities

The mortality and deformity data for the larvae used for the proteomics assay was already presented (submitted manuscript; Supplementary file 1): no significant effects were detected compared to the DMSO control group. In the larvae used for the metabolomics assay, none of the PAHs significantly increased the mortality after 14 days of exposure (FE, $p > 0.05$, data not shown). The highest observed mortality was equal to 9.44% (5.98-14.92) in the group of larvae

exposed to retene (% mortality and 95% confidence interval). The mortality of the control group (exposed to DMSO only) was 4.44% (2.27-8.52). None of the tested PAHs had a significant effect on the BSD severity index (KW, $p > 0.05$). This index ranged from 0.06 ± 0.05 (control group) to 0.15 ± 0.13 (retene) across all treatments (mean ± SD).

3.2. Water parameters and PAH concentrations

The characteristics of the lake water used in the metabolomics assay were as follows: conductivity 26.2 ± 1.0 µS, pH 7.24 ± 0.13, temperature 11.5 ± 0.3°C and oxygen saturation >96%. The water parameters for the proteomics assay experiments have already been presented (submitted manuscript; Supplementary file 1) and were very similar to those presented above. Similarly, the concentrations of each PAH in water at different time points in the proteomics assay experiments have been presented separately (submitted manuscript; Supplementary file 1). Due to some water samples storage issues, it was only possible to measure the concentrations of pyrene in the metabolomics assay experiment. The concentration of pyrene in the tanks left without fish was 10.45 ± 2.61 $\mu g.L^{-1}$ (Fig. 1A), close to what was measured in the proteomics assay experiments, i.e. 8.84 ± 1.99 $\mu g.L^{-1}$ (submitted manuscript; Supplementary file 1). As observed previously in the proteomics assay experiments (submitted manuscript; Supplementary file 1), the concentration of pyrene measured in the water in the presence of larvae tended to decrease over time (Fig. 1A). The average fluorescence spectrums for pyrene in the exposure water are displayed in figure 1B. No metabolites were detected in the tanks without larvae, while one peak of metabolite was detected (around 340 nm) already after 1 day of exposure in the presence of larvae. This peak of metabolite was noticeably higher after 3, 7 and 10 days of exposure, and then further increased after 14 days. Unlike in the proteomics assay experiments

(submitted manuscript; Supplementary file 1), it was unclear if another peak could be observed around 360 nm.

3.3. Proteomics analysis output

A total of 28 proteins were differentially expressed in the hearts of rainbow trout larvae after 7 days of exposure to retene, pyrene or phenanthrene (Fig. 2). The raw output from the DEP package analysis for those proteins, including all *p*-values and $\log_2$ fold changes, is available in the Supplementary file 2. Some proteins such as cytochrome P450 and sulfotransferase were identified twice in the RefSeq database, most likely because different isoforms of the same proteins were differentially expressed by one or several of the tested PAHs. The cytochrome P450 with the highest fold change values was the only protein that was significantly differentially expressed by all PAHs, while the uncharacterized protein displayed in figure 2 was significantly affected by both retene and pyrene. This uncharacterized protein showed similarity with the MAdCAM-1 protein (mucosal vascular addressin cell adhesion molecule 1, also known as addressin), according to BLASTp. All other proteins were significantly differentially expressed by only one PAH, despite some relatively high measured fold changes like in the case of the other cytochrome P450 isoform following exposure to pyrene, for example. High variably between replicates can explain those observations. In addition to those 28 proteins, one differentially expressed protein was found exclusively when using the *S. salar* database during the bioinformatics analyses: DNA (cytosine-5)-methyltransferase was significantly upregulated by phenanthrene only ($\log_2$-FC = 0.74, Supplementary file 2).

A total of 43 proteins were differentially expressed in the hearts of rainbow trout larvae after 14 days of exposure to retene, pyrene or phenanthrene (Fig. 3), in addition to 11 proteins identified only when using the *S. salar* database during the bioinformatics analyses (Fig. 4). The raw output

from the DEP package analysis for those proteins, including all *p*-values and $\log_2$ fold changes, is available in the Supplementary file 2. Only three proteins were differentially expressed by all compounds after 14 days of exposure: the cytochrome P450 isoform with the highest fold change values, UDP-glucuronosyltransferase-like (Fig. 3) and the protein TFG isoform X4 (Fig. 4). One of the sulfotransferase isoforms as well as the UTP—glucose-1-phosphate uridylyltransferase were significantly upregulated by both retene and phenanthrene (Fig. 3). Those two compounds also had in common the significant depletion of several proteins: smoothelin-like protein 2, ER membrane protein complex subunit 2-like, high mobility group protein B1, fatty acid-binding protein (heart-like) and 60S ribosomal protein L22-like isoform X2 (Fig. 3 and 4). The protein tubulin-folding cofactor B was significantly depleted by both pyrene and retene (Fig. 3). All other proteins were significantly differentially expressed by only one PAH. The BLASTp search suggested that the uncharacterized protein displayed in figure 3 is similar to the Rapunzel protein. Overall, only 4 proteins were found to be differentially expressed after both 7 and 14 days of exposure: cytochrome P450 (both isoforms), hemopexin, sulfotransferase (both isoforms) and UDP-glucuronosyltransferase-like. Since the hemopexin protein was identified in the *O. mykiss* database only after 7 days and in the *S. salar* database only after 14 days, it is possible that those are two different isoforms.

3.4. Metabolomics analysis output

A total of 69 identified metabolites were measured and included in the analyses. None of the metabolites were significantly enriched or depleted in the hearts of rainbow trout larvae exposed to retene for 14 days (Fig. 5). Significantly enriched or depleted metabolites were only detected following exposure to pyrene or phenanthrene, and only octadecane-1-ol (stearyl alcohol) was significantly depleted by both PAHs. Overall, a very high variability was observed in the data

among replicates for several metabolites. This can easily be seen in the volcano plots (Fig. 5) as several metabolites had a relatively high (or low) $\log_2$ fold change value but were still not significantly different when compared to the DMSO control group (with low $-\log_{10}$ adjusted *p*-values) following the LIMMA analysis. Finally, it is worth mentioning that phenanthrene itself was detected in each of the four replicate samples of the hearts of the rainbow trout larvae exposed to phenanthrene, but not in any other exposure group (controls, retene or pyrene). Retene and pyrene were not detected in any sample. The raw output from the DEP package analysis for all metabolites, including all *p*-values and $\log_2$ fold changes, is available in the Supplementary file 3.

3.5. Pathway enrichment analysis

Significantly enriched KEGG pathways are presented in the Table 1. The only pathways common to every tested compound as well as both sampling points were related to metabolism of xenobiotics, retinol metabolism and steroid hormone biosynthesis, and were linked mostly to two proteins: cytochrome P450 and UDP-glucuronosyltransferase. Overall, those two proteins were present in the majority of the enriched pathways. A few interesting pathways were included in the presented data despite only having *p*-values close to the significance level. Several complete KEGG pathways of interest are available in Supplementary files 4 and 5.

Very few relevant metabolites were involved in the presented pathways. Arabitol was the only significantly altered metabolite (Fig. 5) present in an enriched pathway, i.e. the pentose and glucuronate interconversions pathway in the case of phenanthrene. Phenylalanine was present in two pathways altered by phenanthrene (dre00360 and dre00400), but was not significant itself in the metabolite dataset (Fig. 5) despite a relatively high fold change value ($\log_2$-FC = 0.55) (Supplementary file 5E).

4. Discussion

4.1. Effects of PAHs on larvae development and concentrations of PAHs in water

None of the three model PAHs significantly increased the mortality or the BSD index in the rainbow trout larvae used for the metabolomics assay. This is very consistent with the results of the transcriptomics and proteomics assays (Supplementary file 1). The concentration of pyrene over time in the metabolomics assay exposure followed a similar trend as that reported for the transcriptomics assay, and its concentration in the tank without larvae was close to the one previously reported (submitted manuscript; Supplementary file 1). However, several differences were observed in the magnitude of the peaks of the first metabolite appearing at 342 nm (speculated as being either 1-hydroxypyrene glucuronide or 1-hydroxypyrene) between the two studies, especially at 7 and 14 days (submitted manuscript; Supplementary file 1). These may be a result of subtle biological differences between larvae, as the ones used for the transcriptomics assay and the metabolomics assays were from two different batches and used in two distinct experiments. Experiments involving the quantification of pyrene and its metabolites in both larvae and exposure water using a more sensitive HPLC method are currently underway.

4.2. PAHs cause distinct changes on the cardiac proteome

Overall, very few proteins were differentially expressed by more than one PAH, suggesting that each PAH caused unique changes in the cardiac proteome of the rainbow trout ELS. The proteins that were altered by all three compounds were mostly related to the metabolism of xenobiotics, i.e. cytochrome P450 and UDP-glucuronosyltransferase. It was well translated into the PEAs as well, with those two proteins being the only ones involved in metabolic pathways common to all three PAHs (Table 1). This also suggests that each PAH was able to activate the AhR. These

phase I and II metabolism proteins as well as sulfotransferase and hemopexin were also the only proteins altered at both sampling time points. Retene was the most potent cytochrome P450 and UDP-glucuronosyltransferase inducer, as well as the only compound to induce another cytochrome P450 isoform at significant levels. Phenanthrene had no significant effect on UDP-glucuronosyltransferase after 7 days but was able to induce it after 14 days. Retene was also the only compound to induce sulfotransferase, with the exception of phenanthrene also inducing one of the two identified isoforms after 14 days. Unique signatures from each PAH were also observed in the cardiac transcriptome, as well as similar expression patterns for the genes encoding for the aforementioned proteins involved in the metabolism of xenobiotics (submitted manuscript). Unique proteomic fingerprints were already described *in vitro* between different PAHs or PAHs mixtures (Hooven and Baird, 2008). Pyrene and phenanthrene were equipotent to significantly induce the protein level of the first isoform of cytochrome P450 after 14 days of exposure (Fig. 3 and Supplementary file 2), but otherwise showed a different proteomic fingerprint. This suggest that for weak AhR agonists such as these two compounds, their toxicity cannot be predicted based on their ability to activate the AhR pathway.

High conservation between responses at the gene or protein expression levels has already been reported before for various model AhR agonists in another fish species (whole body tissue), the white sturgeon (*Acipenser transmontanus*) (Doering et al., 2016). At the transcriptomic level, retene altered the expression of several genes involved in the generation of the cardiac action potential, ion homeostasis (including calcium) and the sarcomere (actin, myosin and troponin) at different time points of the early heart development (submitted manuscript). However, as most of these changes at the gene expression level were observed much earlier during development (i.e. after 1 and 3 days of exposure), it is possible that the present proteomics assay conducted after 7

and 14 days of exposure missed most of the relevant changes at the protein level. A similar remark can be made for pyrene, which was found to alter several myosin-related genes after 1 day of exposure (submitted manuscript). Performing proteomics on the cardiac tissue of rainbow trout larvae exposed to those two PAHs for 1 or 3 days is technically feasible, but would require more time, skilled manpower and resources, as it would require more than 45 individual hearts being dissected and pooled per sample.

Nonetheless, concomitant results can be highlighted from the proteomics data from the present study. Retene depleted proteins such as calreticulin after 7 days, as well as alpha-actinin-1 (not significant), tropomyosin alpha-4 and myosin-11 after 14 days. Interestingly, calreticulin is a protein of similar function as calsequestrin, as both are involved in the storage of calcium in the endoplasmic reticulum for the former and in the sarcoplasmic reticulum for the latter (Lee and Michalak, 2010). Retene was already downregulating the expression of at least one gene related to calsequestrin (*casq1b*) in the rainbow trout developing heart (submitted manuscript). Calcium homeostasis is a known target of PAHs mixture in fish (Greer, J. B. et al., 2019; Xu et al., 2016; Xu et al., 2019). The present study suggests that retene is also able to alter calcium storage and homeostasis by reducing the calreticulin content at the protein level. While it is calsequestrin and not calreticulin that is known to play a direct role in the control of excitation-contraction coupling of cardiomyocytes, recent studies in mice suggests that calreticulin-dependent homeostasis of calcium is also important to maintain the normal physiological function of the heart. Calreticulin may indirectly affect the calcium cycling-proteins and gap junctions of the sarcoplasmic reticulum (Lee et al., 2013). Another interesting protein affected by retene in regards to calcium handling is the peptidylpropyl isomerase, which was significantly depleted after 14 days of exposure (Fig. 4). The gene encoding for the peptidylpropyl isomerase 1 (*Pin1*)

was shown to play a role in calcium handling in mice cardiomyocytes, by influencing the SERCA (sarco/endoplasmic reticulum Ca^{2+}-ATPase) pump and the NCX1 (sodium/calcium) exchanger protein levels (Sacchi et al., 2017). The alteration of proteins related to calcium handling and myocardium architecture (including one tropomyosin isoform) was already reported in the adult heart of zebrafish exposed to the highly potent AhR agonist TCDD (Zhang, J. et al., 2013).

Two very important KEGG pathways in regards to the cardiac function appeared to be altered by retene: vascular smooth muscle contraction (although only close to be significant, $p = 0.07$, Supplementary file 4A) at day 7 and tight junctions at day 14 (Supplementary file 5C). Several proteins related to myosins appeared to be depleted in both pathways (although not always significantly). Again, comparable results were found in our transcriptomic assay, as several genes related to myosins or claudins (key components of tight junctions) were significantly altered by retene (submitted manuscript). The only protein significantly altered in the case of the vascular smooth muscle contraction pathway was one isoform of the Rho guanine nucleotide exchange factor 1. Guanine nucleotide exchange factors (GEFs) are known to play key roles in the angiogenesis and the regulation of the vascular function (Kather and Kroll, 2013). Another notable protein highly depleted by retene was similar to the junctional adhesion molecule C. Involved in tight junctions, junctional adhesion molecules play important roles in the angiogenesis and the regulation of vascular permeability in mammals (Weber et al., 2007).

Retene is known to induce oxidative stress and DNA damage (Maria et al., 2005; Peixoto et al., 2019). In the present study, retene was the only PAH to significantly induce the superoxide dismutase protein in the cardiac tissue, probably as a response to an increased content in reactive oxygen species (ROS). Retene also depleted several proteins involved in DNA damage repair

519 (Supplementary file 5A) and altered the level of several proteins in the FoxO signaling pathway
520 (Supplementary file 5B), including the 5'-AMP-activated protein kinase subunit beta 1 (log_2-FC
521 = -1.20) related to the AMPK enzyme. In mammalian cells, the FoxO signaling pathway is
522 known to play a role in DNA damage repair, especially via the FOXO3 transcription factor
523 (Bigarella et al., 2017; Tran et al., 2002). AMPK has also been shown to interact with FOXO3 in
524 mechanisms of defense against oxidative stress (Greer, E. L. et al., 2007; Li et al., 2009).
525 Although our data may suggest that retene could promote DNA damage not only by inducing
526 oxidative stress but also by altering the AMPK enzyme and other proteins involved in DNA
527 repair, more research is needed to explore that hypothesis.

528 Both retene and pyrene significantly reduced the protein level of tubulin-folding cofactor B (Fig.
529 3). Tubulin-folding cofactors control the availability of tubulin subunits in eukaryotic cells
530 (Szymanski, 2002). Retene also slightly but significantly reduced the protein level of tubulin beta
531 chain (also known as beta tubulin) (Fig. 3). The present study is not the first to report such
532 findings for PAHs. Tubulins alpha and beta protein levels were altered *in vitro* following
533 exposure to benzo[a]pyrene, dibenzo[a,l]pyrene or coal tar extract (Hooven and Baird, 2008).
534 Interestingly, beta tubulin has been shown to play a role in the AhR function in mammalian cells:
535 it could reduce the binding of the AhR/Arnt (Ah receptor nuclear translocator) heterodimer to the
536 DRE (dioxin response element) by interacting with Arnt but not the AhR (Zhang, T. et al., 2010).
537 One can hypothesize that a reduced beta tubulin biosynthesis or protein level could result in the
538 opposite effect, i.e. an increased binding of the heterodimer with the DRE. Additional research in
539 fish regarding the role of beta tubulin is needed to explore that hypothesis, as well as its relative
540 importance in the regulation of the AhR-mediated toxicity of PAHs.

At the transcriptomic level, pyrene disrupted the expression of multiple genes involved in the myosin complex as early as after 24 hours of exposure, and in an opposite way compared to retene (submitted manuscript). In the present work, pyrene depleted alpha-actinin-1 after 14 days of exposure (Fig. 3), as well as myosin-11, but the trend was not significant for the latter. In vertebrates, alpha-actinin 2 and 3 are the two muscular forms of actinin, while alpha-actinin 1 and 4 are more broadly expressed (Holterhoff et al., 2009). Those non-muscle forms of alpha-actinin not only bind with actin, but also play a role in stress fibers, focal adhesions, the cytoskeleton, as well as in adherens and tight junctions (Otey and Carpen, 2004). The adherens junction KEGG pathway was indeed close to being significantly enriched following the PEAs (p =0.06, Table 1). This pathway involved not only alpha-actinin-1, but also a protein similar to catenin delta-1, which had a relatively highly negative log2-FC value (-0.97, data not shown) but was not significantly depleted. The alteration of proteins related to myosin, actin, tropomyosin or more generally to the muscular system development and function was already reported for fish exposed to PAHs mixtures (Bohne-Kjersem et al., 2010; Karlsen et al., 2011; Simmons and Sherry, 2016). Our data suggest that both retene and pyrene alone are able to alter such proteins. Early exposure to these PAHs could result in a loss in cardiac fitness later in the life of the juvenile fish, as demonstrated with PAHs mixture in several fish species (Hicken et al., 2011; Incardona et al., 2015).

The most interesting changes in protein expression linked to the pyrene exposure were related to the metabolism and handling of iron. Iron-mediated oxidation-reduction reactions are required for the proper metabolism of oxygen in the heart. Iron levels in the heart are tightly regulated, and consequently heart failure is a common denominator in conditions of systemic iron imbalance (Lakhal-Littleton, 2019). In the present study, pyrene significantly depleted

564 hemopexin from the cardiac tissue of the exposed rainbow trout larvae, especially after 7 days of
565 exposure (Fig. 2). Hemopexin is a plasma protein with a very high binding affinity for heme
566 complexes (cytochromes, iron and porphyrin complexes), and it plays a protective role against
567 heme-induced oxidative stress (Ingoglia et al., 2017; Tolosano and Altruda, 2002). Altered gene
568 expression or protein levels for hemopexin were already reported in several studies involving
569 different fish species exposed to benzo[a]pyrene or complex PAHs mixtures (Alderman et al.,
570 2017; Bohne-Kjersem et al., 2009; Enerstvedt et al., 2017; Karlsen et al., 2011; Won et al.,
571 2013). Interestingly, pyrene was also able to increase the expression of several proteins involved
572 in porphyrin metabolism (Supplementary file 4B), notably uroporphyrinogen decarboxylase
573 (UROD) which was also upregulated at the transcriptomic level after 7 days of exposure in our
574 related study (submitted manuscript). Finally, several proteins involved in the ferroptosis
575 pathway (Supplementary file 4D) and most notably ferritin were also enriched following
576 exposure to pyrene, suggesting a response to an increase in free iron ion content. It is worth
577 mentioning that pyrene also upregulated two genes related to the hemoglobin complex, *hbae1.3*
578 and *hbae3*, as well as two genes linked to ferritin and transferrin, in the aforementioned
579 transcriptomic study. In fish, PAHs mixtures have been previously shown to alter the protein
580 levels of hemoglobin and other proteins involved in iron metabolism (Pampanin et al., 2014).

581 Phenomenon such as hemolysis (destruction of red blood cells) are known to release hemoglobin
582 and free heme into the circulation. Free toxic hemes are generally scavenged by hemopexin and
583 subsequently catabolized into carbon monoxide (CO), biliverdin, and ferrous iron (Fe^{2+}) by heme
584 oxygenase-1 (HO-1). In severe hemolysis, the extensive release of heme from hemoglobin or
585 decreased hemopexin levels lead to an increase in the iron level in the circulation, which is
586 consequently handled by ferritin (Chiang et al., 2019; NaveenKumar et al., 2018). In the present

study, pyrene clearly appeared to act as a disruptor of heme and iron metabolism in the rainbow trout ELS heart, although the exact triggering mechanisms remains to be found. In birds exposed to PAHs, metabolism of parent PAHs by CYP1A creates oxidative PAH metabolites that cause oxidative damage to erythrocytes, resulting in hemolytic anemia associated with an increase in ferritin (Troisi et al., 2007). Hemolytic anemia following exposure to naphthalene or complex PAHs mixtures has also been reported *in vitro* for mammals (Couillard and Leighton, 1993). Interestingly, genes coding for HO-1 and hemopexin are AhR-regulated genes, and an *in vitro* exposure of human liver cells to benzo[a]pyrene resulted in a decreased hemopexin gene expression (Iwano et al., 2010).

Phenanthrene appeared to be the least potent of all three tested PAHs in regards to changes in the cardiac proteome after 7 days. Besides the significant induction of cytochrome P450, one of the most notable change was the depletion of both alpha and beta fibrinogen chains (Fig. 2). Fibrinogen is important to heal tissue and blood vessels injuries, as it forms fibrin-based blood clots following enzymatic conversion by thrombin. A reduced fibrinogen content in larvae exposed to phenanthrene could indicate a reduced ability to recover from such damage, or a response to tissue and vascular damage potentially caused by phenanthrene. Proteins involved in the fibrinolytical system (including fibrinogen) were altered in the juvenile cod (*Gadus morhua*) exposed to a complex PAHs mixture (Bohne-Kjersem et al., 2009). After 14 days, phenanthrene had in common with retene the significant depletion of smoothelin (Fig. 3), a protein found in vascular smooth muscles that has been shown to interact with calmodulin and troponin (Ulke-Lemée et al., 2017). In mammals, a deficiency in smoothelin has been associated with reduced vascular contractility, and is often observed after vascular damages (Rensen et al., 2008; van Eys et al., 2007). Another protein significantly depleted by both retene and phenanthrene after 14

610 days of exposure was the heart-like fatty acid-binding protein (Fig. 3), a protein responsible of
611 the intracellular transportation of long-chain fatty acid and found in abundance in
612 cardiomyocytes (Schaap et al., 1998). Some proteins involved in the metabolism of fatty acids
613 were also significantly altered by phenanthrene, i.e. long-chain-fatty-acid—CoA ligase 1-like
614 and aldehyde dehydrogenase family 16 member A1 (Fig. 3 and Table 1). Fatty acids are an
615 important source of energy for the heart, and our data suggest that phenanthrene might affect
616 both their transport and metabolism. Aldehyde dehydrogenase, heart-like fatty acid-binding
617 protein as well pyruvate dehydrogenase were all significantly altered by phenanthrene (Fig. 3),
618 which is consistent with the results reported in the liver proteome of the largemouth bass
619 (*Micropterus salmoides*) exposed to phenanthrene too (Sanchez et al., 2009). Pyruvate
620 dehydrogenase catalyzes the oxidative decarboxylation of pyruvate generated from glycolysis,
621 producing NADH, carbon dioxide and acetyl coenzyme A (acetyl-CoA). It is an essential link
622 between the glycolysis and the TCA cycle located in the mitochondria, and plays an important
623 role in the oxidative consumption of glucose (Tzagoloff, 2012).

624 4.3. Changes induced in the metabolites profile of the rainbow trout heart

625 No significant changes were observed for any of the measured metabolites following exposure to
626 retene (Fig. 5). Overall, a very high variability was observed in the data among replicates for
627 several metabolites and for all compounds. Increasing the sample size (N = 4) would have
628 probably helped to detect more changes in the cardiac metabolome in the present study. Even
629 though several metabolites were either significantly depleted or enriched in the hearts of pyrene
630 or phenanthrene-treated larvae, very few could be linked to the proteomics datasets and mapped
631 into any KEGG pathways following the PEAs, making the interpretation of our datasets difficult.
632 The only significant metabolite mapped to a KEGG pathway was arabitol, and was in excess

633 after exposure to phenanthrene and involved in the pentose and glucuronate interconversions
634 pathway as well (Fig. 5 and Table 1). The slight but significant valine deficiency observed for
635 the phenanthrene exposure (Fig. 5) could be indicative of a disorder in the catabolism of that
636 particular BCAA (branched-chain amino acids). Altered or defective BCAA catabolism can
637 potentially be linked to heart failure (Sun, H. and Wang, 2016). Another interesting enriched
638 metabolite in the case of phenanthrene was phenylalanine. It was associated to a significant
639 induction of the expression of one aspartate aminotransferase (also known as aspartate
640 transaminase) isoform (Supplementary file 5E), which catalyzes the transformation of
641 phenylalanine to phenylpyruvate. However, even though phenylalanine had a relatively high fold
642 change, it was not significantly enriched according to the metabolomics data analyses, making it
643 difficult to draw any conclusions about it.

644 Myo-inositol (often simply referenced as inositol) was slightly but significantly in excess in the
645 cardiac tissue of rainbow trout ELS following pyrene exposure. Inositol is an important basis for
646 several secondary messengers such as inositol trisphosphate, which for example plays important
647 roles in the calcium homeostasis of cardiomyocytes (Garcia and Boehning, 2017). More research
648 is needed to assess if pyrene can possibly affect the cardiac function by altering the inositol
649 signaling pathway. Alanine content was significantly lowered by pyrene in the cardiac tissue
650 compared to control larvae. Alanine is an important amino acid for protein biosynthesis, but is
651 also used as an alternative source of energy by being converted into pyruvate (used to produce
652 glucose) in the liver or in muscles. Low levels in alanine could thus indicate an increased energy
653 demand or an altered glucose cycle in the cardiac tissue of larvae exposed to pyrene. Pantothenic
654 acid, also known as vitamin B_5, appeared to be in slight excess following exposure to pyrene.
655 Pantothenic acid is required for the biosynthesis of coenzyme A (CoA), which is involved in

various key biological processes such as the oxidation of fatty acids, carbohydrates, pyruvate, lactate, ketone bodies, and amino acids, as well as many other biosynthesis reactions (Tahiliani and Beinlich, 1991). An excess in pantothenic acid could mean an altered CoA synthesis and thus possible repercussions on all the aforementioned biological processes.

4. Conclusion

This study highlights some possible mechanisms of cardiotoxicity of retene and pyrene in fish ELS. Retene altered several key proteins related to muscle contraction, cellular tight junctions or calcium homeostasis. Those observations are very consistent with some results that we obtained at the transcriptomic level (submitted manuscript), where retene was found to alter numerous genes linked to key cardiac ion channels, the sarcomere or intercellular junctions. The most notable finding of the present study was the ability of pyrene alone to disrupt the levels of several proteins linked with the metabolism and handling of iron and heme. While such mechanisms have been mentioned already in the literature for fish or birds exposed to PAHs mixtures or benzo[a]pyrene, our data suggests that pyrene, one of the most widespread PAH in the environment, could be an important contributor to this toxic pathway. More research is needed to confirm that hypothesis, as well as to determine if those changes are happening directly (i.e. activation of the AhR by pyrene) or indirectly (i.e. for example via hemolysis induced by oxidative stress). As observed at the transcriptomic level, no clear mechanisms or pathways critically relevant to the fish ELS cardiac function could be highlighted for phenanthrene.

Acknowledgements

This study was funded by the Academy of Finland (projects 285296, 294066 and 319284 to Eeva-Riikka Vehniäinen). We are very grateful to Mervi Koistinen, Terhi Rahkonen, Jaakko Litmanen as well as the staff of the Konnevesi Research Station for their technical assistance. Mass spectrometry analyses were performed at the Turku Proteomics Facility, supported by Biocenter Finland.

Data accessibility statement

The mass spectrometry proteomics data have been deposited to the ProteomeXchange Consortium via the PRIDE partner repository with the dataset identifier PXD017294.

Author contributions

Cyril Rigaud: Conceptualization, Methodology, Data Acquisition, Data Analysis, Writing – Original Draft. **Andreas Eriksson:** Conceptualization, Methodology, Data Acquisition, Data Analysis, Writing – Review & Editing. **Anne Rokka:** Methodology, Data Acquisition, Writing – Review & Editing. **Morten Skaugen:** Methodology, Data Acquisition, Data Analysis. **Jenna Lihavainen:** Methodology, Data Acquisition, Writing – Review & Editing. **Markku Keinänen:** Methodology. **Heli Lehtivuori:** Methodology. **Eeva-Riikka Vehniäinen:** Conceptualization, Methodology, Funding Acquisition, Project Administration, Supervision, Writing – Review & Editing.

REFERENCES

Ahad JM, Jautzy JJ, Cumming BF, Das B, Laird KR, Sanei H, 2015. Sources of polycyclic aromatic hydrocarbons (PAHs) to northwestern Saskatchewan lakes east of the Athabasca oil sands. Org Geochem. 80, 35-45.

Alderman SL, Dindia LA, Kennedy CJ, Farrell AP, Gillis TE, 2017. Proteomic analysis of sockeye salmon serum as a tool for biomarker discovery and new insight into the sublethal

toxicity of diluted bitumen. Comparative Biochemistry and Physiology Part D: Genomics and Proteomics. 22, 157-66.

Andersson JT, Achten C, 2015. Time to say goodbye to the 16 EPA PAHs? Toward an up-to-date use of PACs for environmental purposes. Polycyclic Aromatic Compounds. 35, 330-54.

Anyakora C, Ogbeche A, Palmer P, Coker H, 2005. Determination of polynuclear aromatic hydrocarbons in marine samples of Siokolo Fishing Settlement. Journal of chromatography A. 1073, 323-30.

Barjhoux I, Cachot J, Gonzalez P, Budzinski H, Le Menach K, Landi L, Morin B, Baudrimont M, 2014. Transcriptional responses and embryotoxic effects induced by pyrene and methylpyrene in Japanese medaka (*Oryzias latipes*) early life stages exposed to spiked sediments. Environmental Science and Pollution Research. 21, 13850-66.

Barron MG, Heintz R, Rice SD, 2004. Relative potency of PAHs and heterocycles as aryl hydrocarbon receptor agonists in fish. Marine Environmental Research. 58, 95-100.

Bigarella CL, Li J, Rimmelé P, Liang R, Sobol RW, Ghaffari S, 2017. FOXO3 transcription factor is essential for protecting hematopoietic stem and progenitor cells from oxidative DNA damage. J Biol Chem. 292, 3005-15.

Billiard SM, Querbach K, Hodson PV, 1999. Toxicity of retene to early life stages of two freshwater fish species. Environmental Toxicology and Chemistry: An International Journal. 18, 2070-7.

Bohne-Kjersem A, Bache N, Meier S, Nyhammer G, Roepstorff P, Sæle Ø, Goksøyr A, Grøsvik BE, 2010. Biomarker candidate discovery in Atlantic cod (*Gadus morhua*) continuously exposed to North Sea produced water from egg to fry. Aquatic toxicology. 96, 280-9.

Bohne-Kjersem A, Skadsheim A, Goksøyr A, Grøsvik BE, 2009. Candidate biomarker discovery in plasma of juvenile cod (*Gadus morhua*) exposed to crude North Sea oil, alkyl phenols and polycyclic aromatic hydrocarbons (PAHs). Mar Environ Res. 68, 268-77.

Brette F, Shiels HA, Galli GLJ, Cros C, Incardona JP, Scholz NL, Block BA, 2017. A novel cardiotoxic mechanism for a pervasive global pollutant. Scientific reports. 7, 41476.

Chiang S, Chen S, Chang L, 2019. A dual role of Heme Oxygenase-1 in cancer cells. International journal of molecular sciences. 20, 39.

Couillard CM, Leighton FA, 1993. In vitro red blood cell assay for oxidant toxicity of petroleum oil. Environmental Toxicology and Chemistry: An International Journal. 12, 839-45.

Cox J, Mann M, 2008. MaxQuant enables high peptide identification rates, individualized ppb-range mass accuracies and proteome-wide protein quantification. Nat Biotechnol. 26, 1367.

Cox J, Neuhauser N, Michalski A, Scheltema RA, Olsen JV, Mann M, 2011. Andromeda: a peptide search engine integrated into the MaxQuant environment. Journal of proteome research. 10, 1794-805.

Cypher AD, Consiglio J, Bagatto B, 2017. Hypoxia exacerbates the cardiotoxic effect of the polycyclic aromatic hydrocarbon, phenanthrene in *Danio rerio*. Chemosphere. 183, 574-81.

Doering JA, Hecker M, Villeneuve D, Zhang X, 2019. Adverse Outcome Pathway on aryl hydrocarbon receptor activation leading to early life stage mortality, via increased COX-2.

Doering JA, Tang S, Peng H, Eisner BK, Sun J, Giesy JP, Wiseman S, Hecker M, 2016. High conservation in transcriptomic and proteomic response of white sturgeon to equipotent concentrations of 2, 3, 7, 8-TCDD, PCB 77, and benzo[a]pyrene. Environ Sci Technol. 50, 4826-35.

Eggleton J, Thomas KV, 2004. A review of factors affecting the release and bioavailability of contaminants during sediment disturbance events. Environ Int. 30, 973-80.

Enerstvedt KS, Sydnes MO, Pampanin DM, 2017. Study of the plasma proteome of Atlantic cod (*Gadus morhua*): Effect of exposure to two PAHs and their corresponding diols. Chemosphere. 183, 294-304.

Garcia MI, Boehning D, 2017. Cardiac inositol 1,4,5-trisphosphate receptors. Biochimica et Biophysica Acta (BBA)-Molecular Cell Research. 1864, 907-14.

Gatto L, Lilley KS, 2011. MSnbase-an R/Bioconductor package for isobaric tagged mass spectrometry data visualization, processing and quantitation. Bioinformatics. 28, 288-9.

Geier MC, Minick DJ, Truong L, Tilton S, Pande P, Anderson KA, Teeguardan J, Tanguay RL, 2018. Systematic developmental neurotoxicity assessment of a representative PAH Superfund mixture using zebrafish. Toxicol Appl Pharmacol. 354, 115-25.

Greer EL, Oskoui PR, Banko MR, Maniar JM, Gygi MP, Gygi SP, Brunet A, 2007. The energy sensor AMP-activated protein kinase directly regulates the mammalian FOXO3 transcription factor. J Biol Chem. 282, 30107-19.

Greer JB, Pasparakis C, Stieglitz JD, Benetti D, Grosell M, Schlenk D, 2019. Effects of corexit 9500A and Corexit-crude oil mixtures on transcriptomic pathways and developmental toxicity in early life stage mahi-mahi (*Coryphaena hippurus*). Aquatic Toxicology. 212, 233-40.

Gündel U, Kalkhof S, Zitzkat D, von Bergen M, Altenburger R, Küster E, 2012. Concentration–response concept in ecotoxicoproteomics: Effects of different phenanthrene concentrations to the zebrafish (*Danio rerio*) embryo proteome. Ecotoxicology and Environmental Safety. 76, 11-22.

765 Hendon LA, Carlson EA, Manning S, Brouwer M, 2008. Molecular and developmental effects of
766 exposure to pyrene in the early life-stages of *Cyprinodon variegatus*. Comparative Biochemistry
767 and Physiology Part C: Toxicology & Pharmacology. 147, 205-15.

768 Hernández-de-Diego R, Tarazona S, Martínez-Mira C, Balzano-Nogueira L, Furió-Tarí P,
769 Pappas Jr GJ, Conesa A, 2018. PaintOmics 3: a web resource for the pathway analysis and
770 visualization of multi-omics data. Nucleic Acids Res. 46, W503-9.

771 Hicken CE, Linbo TL, Baldwin DH, Willis ML, Myers MS, Holland L, Larsen M, Stekoll MS,
772 Rice SD, Collier TK, 2011. Sublethal exposure to crude oil during embryonic development alters
773 cardiac morphology and reduces aerobic capacity in adult fish. Proceedings of the National
774 Academy of Sciences. 108, 7086-90.

775 Hiller K, Hangebrauk J, Jäger C, Spura J, Schreiber K, Schomburg D, 2009. MetaboliteDetector:
776 comprehensive analysis tool for targeted and nontargeted GC/MS based metabolome analysis.
777 Anal Chem. 81, 3429-39.

778 Holterhoff CK, Saunders RH, Brito EE, Wagner DS, 2009. Sequence and expression of the
779 zebrafish alpha-actinin gene family reveals conservation and diversification among vertebrates.
780 Developmental dynamics: an official publication of the American Association of Anatomists.
781 238, 2936-47.

782 Honkanen JO, Rees CB, Kukkonen JV, Hodson PV, 2020. Temperature determines the rate at
783 which retene affects trout embryos, not the concentration that is toxic. Aquatic Toxicology,
784 105471.

785 Hooven LA, Baird WM, 2008. Proteomic analysis of MCF-7 cells treated with benzo[a]pyrene,
786 dibenzo[a, l]pyrene, coal tar extract, and diesel exhaust extract. Toxicology. 249, 1-10.

787 Hummel J, Selbig J, Walther D, Kopka J. The Golm Metabolome Database: a database for GC-
788 MS based metabolite profiling. In: Anonymous . Metabolomics: Springer; 2007. p. 75-95.

789 Incardona JP, Carls MG, Hiroki T, Sloan CA, Collier TK, Scholz NL, 2005. Aryl hydrocarbon
790 receptor–independent toxicity of weathered crude oil during fish development. Environ Health
791 Perspect. 113, 1755-62.

792 Incardona JP, Carls MG, Holland L, Linbo TL, Baldwin DH, Myers MS, Peck KA, Tagal M,
793 Rice SD, Scholz NL, 2015. Very low embryonic crude oil exposures cause lasting cardiac
794 defects in salmon and herring. Scientific Reports. 5, 13499.

795 Incardona JP, Collier TK, Scholz NL, 2004. Defects in cardiac function precede morphological
796 abnormalities in fish embryos exposed to polycyclic aromatic hydrocarbons. Toxicology and
797 Applied Pharmacology. 196, 191-205.

798 Incardona JP, Gardner LD, Linbo TL, Brown TL, Esbaugh AJ, Mager EM, Stieglitz JD, French
799 BL, Labenia JS, Laetz CA, Tagal M, Sloan CA, Elizur A, Benetti DD, Grosell M, Block BA,

800 Scholz NL, 2014. *Deepwater Horizon* crude oil impacts the developing hearts of large predatory
801 pelagic fish. Proc Natl Acad Sci USA. 111, E1510-8.

802 Ingoglia G, Sag CM, Rex N, De Franceschi L, Vinchi F, Cimino J, Petrillo S, Wagner S,
803 Kreitmeier K, Silengo L, 2017. Hemopexin counteracts systolic dysfunction induced by heme-
804 driven oxidative stress. Free Radical Biology and Medicine. 108, 452-64.

805 Iwano S, Ichikawa M, Takizawa S, Hashimoto H, Miyamoto Y, 2010. Identification of AhR-
806 regulated genes involved in PAH-induced immunotoxicity using a highly-sensitive DNA chip,
807 3D-GeneTM Human Immunity and Metabolic Syndrome 9k. Toxicology in Vitro. 24, 85-91.

808 Kammers K, Cole RN, Tiengwe C, Ruczinski I, 2015. Detecting significant changes in protein
809 abundance. EuPA open proteomics. 7, 11-9.

810 Karlsen OA, Bjørneklett S, Berg K, Brattås M, Bohne-Kjersem A, Grøsvik BE, Goksøyr A,
811 2011. Integrative environmental genomics of cod (*Gadus morhua*): the proteomics approach.
812 Journal of Toxicology and Environmental Health, Part A. 74, 494-507.

813 Kather JN, Kroll J, 2013. Rho guanine exchange factors in blood vessels: fine-tuners of
814 angiogenesis and vascular function. Exp Cell Res. 319, 1289-97.

815 Keith LH, 2015. The source of US EPA's sixteen PAH priority pollutants. Polycyclic Aromatic
816 Compounds. 35, 147-60.

817 Kurek J, Kirk JL, Muir DC, Wang X, Evans MS, Smol JP, 2013. Legacy of a half century of
818 Athabasca oil sands development recorded by lake ecosystems. Proceedings of the National
819 Academy of Sciences. 110, 1761-6.

820 Lakhal-Littleton S, 2019. Mechanisms of cardiac iron homeostasis and their importance to heart
821 function. Free Radical Biology and Medicine. 133, 234-7.

822 Latimer JS, Zheng J. The sources, transport, and fate of PAHs in the marine environment. In:
823 Douben PET, editor. PAHs: An Ecotoxicological Perspective; 2003. p. 7-33.

824 Lee D, Michalak M, 2010. Membrane associated Ca^{2+} buffers in the heart. Biochemistry and
825 Molecular Biology reports.

826 Lee D, Oka T, Hunter B, Robinson A, Papp S, Nakamura K, Srisakuldee W, Nickel BE, Light
827 PE, Dyck JR, 2013. Calreticulin induces dilated cardiomyopathy. PloS one. 8, e56387.

828 Leppänen H, Oikari A, 2001. Retene and resin acid concentrations in sediment profiles of a lake
829 recovering from exposure to pulp mill effluents. J Paleolimnol. 25, 367-74.

830 Li X, Song J, Zhang L, LeMaire SA, Hou X, Zhang C, Coselli JS, Chen L, Wang XL, Zhang Y,
831 2009. Activation of the AMPK-FOXO3 pathway reduces fatty acid–induced increase in
832 intracellular reactive oxygen species by upregulating thioredoxin. Diabetes. 58, 2246-57.

833 Logan DT, 2007. Perspective on ecotoxicology of PAHs to fish. Human and Ecological Risk
834 Assessment: An International Journal. 13, 302-16.

835 Maria VL, Correia AC, Santos MA, 2005. *Anguilla anguilla* L. liver EROD induction and
836 genotoxic responses after retene exposure. Ecotoxicol Environ Saf. 61, 230-8.

837 Maskaoui K, Zhou JL, Hong HS, Zhang ZL, 2002. Contamination by polycyclic aromatic
838 hydrocarbons in the Jiulong River estuary and Western Xiamen Sea, China. Environmental
839 pollution. 118, 109-22.

840 Meriläinen P, Lahdelma I, Oikari L, Hyötyläinen T, Oikari A, 2006. Dissolution of resin acids,
841 retene and wood sterols from contaminated lake sediments. Chemosphere. 65, 840-6.

842 Mu J, Wang J, Jin F, Wang X, Hong H, 2014. Comparative embryotoxicity of phenanthrene and
843 alkyl-phenanthrene to marine medaka (*Oryzias melastigma*). Marine Pollution Bulletin. 85, 505-
844 15.

845 NaveenKumar SK, SharathBabu BN, Hemshekhar M, Kemparaju K, Girish KS, Mugesh G,
846 2018. The role of reactive oxygen species and ferroptosis in heme-mediated activation of human
847 platelets. ACS chemical biology. 13, 1996-2002.

848 Otey CA, Carpen O, 2004. α-actinin revisited: A fresh look at an old player. Cell Motil
849 Cytoskeleton. 58, 104-11.

850 Pampanin DM, Larssen E, Øysæd KB, Sundt RC, Sydnes MO, 2014. Study of the bile proteome
851 of Atlantic cod (*Gadus morhua*): Multi-biological markers of exposure to polycyclic aromatic
852 hydrocarbons. Mar Environ Res. 101, 161-8.

853 Peixoto MS, da Silva Junior, Francisco Carlos, de Oliveira Galvão, Marcos Felipe, Roubicek
854 DA, de Oliveira Alves N, de Medeiros, Silvia Regina Batistuzzo, 2019. Oxidative stress,
855 mutagenic effects, and cell death induced by retene. Chemosphere. 231, 518-27.

856 Rensen S, Niessen P, van Deursen J, Janssen B, Heijman E, Hermeling E, Meens M, Lie N,
857 Gijbels M, Strijkers G, 2008. Smoothelin-B deficiency results in reduced arterial contractility,
858 hypertension, and cardiac hypertrophy in mice. Circulation. 118, 828-36.

859 Rubailo AI, Oberenko AV, 2008. Polycyclic aromatic hydrocarbons as priority pollutants.
860 Journal of Siberian Federal University. Chemistry. 4, 344-54.

861 Ruge Z, Muir D, Helm P, Lohmann R, 2015. Concentrations, trends, and air-water exchange of
862 PAHs and PBDEs derived from passive samplers in Lake Superior in 2011. Environ Sci Technol.
863 49, 13777-86.

864 Sacchi V, Wang BJ, Kubli D, Martinez AS, Jin J, Alvarez Jr R, Hariharan N, Glembotski C,
865 Uchida T, Malter JS, 2017. Peptidyl-prolyl isomerase 1 regulates Ca^{2+} handling by modulating

sarco(endo)plasmic reticulum calcium ATPase and Na^{2+}/Ca^{2+} exchanger 1 protein levels and function. Journal of the American Heart Association. 6, e006837.

Sanchez BC, Ralston-Hooper KJ, Kowalski KA, Inerowicz HD, Adamec J, Sepúlveda MS, 2009. Liver proteome response of largemouth bass (*Micropterus salmoides*) exposed to several environmental contaminants: potential insights into biomarker development. Aquatic toxicology. 95, 52-9.

Schaap FG, van der Vusse, Ger J, Glatz JF. Fatty acid-binding proteins in the heart. In: Anonymous . Cardiac Metabolism in Health and Disease: Springer; 1998. p. 43-51.

Scott JA, Hodson PV, 2008. Evidence for multiple mechanisms of toxicity in larval rainbow trout (*Oncorhynchus mykiss*) co-treated with retene and α-naphthoflavone. Aquatic toxicology. 88, 200-6.

Scott JA, Incardona JP, Pelkki K, Shepardson S, Hodson PV, 2011. AhR2-mediated, CYP1A-independent cardiovascular toxicity in zebrafish (*Danio rerio*) embryos exposed to retene. Aquatic Toxicology. 101, 165-74.

Shen G, Tao S, Wei S, Zhang Y, Wang R, Wang B, Li W, Shen H, Huang Y, Yang Y, 2012. Retene emission from residential solid fuels in China and evaluation of retene as a unique marker for soft wood combustion. Environ Sci Technol. 46, 4666-72.

Shi X, He C, Zuo Z, Li R, Chen D, Chen R, Wang C, 2012. Pyrene exposure influences the craniofacial cartilage development of *Sebastiscus marmoratus* embryos. Mar Environ Res. 77, 30-4.

Simmons DB, Sherry JP, 2016. Plasma proteome profiles of White Sucker (*Catostomus commersonii*) from the Athabasca River within the oil sands deposit. Comparative Biochemistry and Physiology Part D: Genomics and Proteomics. 19, 181-9.

Sun H, Wang Y, 2016. Branched chain amino acid metabolic reprogramming in heart failure. Biochimica et Biophysica Acta (BBA)-Molecular Basis of Disease. 1862, 2270-5.

Sun L, Zuo Z, Chen M, Chen Y, Wang C, 2015. Reproductive and transgenerational toxicities of phenanthrene on female marine medaka (*Oryzias melastigma*). Aquatic Toxicology. 162, 109-16.

Szymanski D, 2002. Tubulin folding cofactors: half a dozen for a dimer. Current Biology. 12, R767-9.

Tahiliani AG, Beinlich CJ. Pantothenic acid in health and disease. In: Anonymous . Vitamins & Hormones: Elsevier; 1991. p. 165-228.

Tolosano E, Altruda F, 2002. Hemopexin: structure, function, and regulation. DNA Cell Biol. 21, 297-306.

Tran H, Brunet A, Grenier JM, Datta SR, Fornace AJ, DiStefano PS, Chiang LW, Greenberg ME, 2002. DNA repair pathway stimulated by the forkhead transcription factor FOXO3a through the Gadd45 protein. Science. 296, 530-4.

Troisi G, Borjesson L, Bexton S, Robinson I, 2007. Biomarkers of polycyclic aromatic hydrocarbon (PAH)-associated hemolytic anemia in oiled wildlife. Environ Res. 105, 324-9.

Tzagoloff A. Mitochondria: Springer Science & Business Media; 2012.

Ulke-Lemée A, Sun DH, Ishida H, Vogel HJ, MacDonald JA, 2017. Binding of smoothelin-like 1 to tropomyosin and calmodulin is mutually exclusive and regulated by phosphorylation. BMC biochemistry. 18, 5.

van Eys GJ, Niessen PM, Rensen SS, 2007. Smoothelin in vascular smooth muscle cells. Trends Cardiovasc Med. 17, 26-30.

Vehniäinen E, Bremer K, Scott JA, Junttila S, Laiho A, Gyenesei A, Hodson PV, Oikari AOJ, 2016. Retene causes multifunctional transcriptomic changes in the heart of rainbow trout (*Oncorhynchus mykiss*) embryos. Environ Toxicol Pharmacol. 41, 95-102.

Vehniäinen E, Haverinen J, Vornanen M, 2019. Polycyclic aromatic hydrocarbons phenanthrene and retene modify the action potential via multiple ion currents in rainbow trout *Oncorhynchus mykiss* cardiac myocytes. Environ Toxicol Chem. 0.

Villalobos SA, Papoulias DM, Meadows J, Blankenship AL, Pastva SD, Kannan K, Hinton DE, Tillitt DE, Giesy JP, 2000. Toxic responses of medaka, d-rR strain, to polychlorinatednaphthalene mixtures after embryonic exposure by in ovo nanoinjection: A partial life-cycle assessment. Environmental toxicology and chemistry. 19, 432-40.

Water Framework Directive, 2000. Directive 2000/60/EC of the European parliament and of the council of 23 October 2000 establishing a framework for community action in the field of water policy. Official Journal of the European Communities. 327, 1-73.

Weber C, Fraemohs L, Dejana E, 2007. The role of junctional adhesion molecules in vascular inflammation. Nature Reviews Immunology. 7, 467.

Wolska L, Mechlińska A, Rogowska J, Namieśnik J, 2012. Sources and fate of PAHs and PCBs in the marine environment. Crit Rev Environ Sci Technol. 42, 1172-89.

Won H, Woo S, Lee A, Yum S, 2013. Gene expression profile changes induced by acute toxicity of benzo[a]pyrene in marine medaka. Toxicology and Environmental Health Sciences. 5, 138-44.

Xu EG, Khursigara AJ, Li S, Esbaugh AJ, Dasgupta S, Volz DC, Schlenk D, 2019. mRNA-miRNA-Seq reveals neuro-cardio mechanisms of crude oil toxicity in red drum (*Sciaenops ocellatus*). Environ Sci Technol. 53, 3296-305.

Xu EG, Mager EM, Grosell M, Pasparakis C, Schlenker LS, Stieglitz JD, Benetti D, Hazard ES, Courtney SM, Diamante G, 2016. Time-and oil-dependent transcriptomic and physiological responses to Deepwater Horizon oil in mahi-mahi (*Coryphaena hippurus*) embryos and larvae. Environ Sci Technol. 50, 7842-51.

Zhang J, Lanham KA, Heideman W, Peterson RE, Li L, 2013. Statistically enhanced spectral counting approach to TCDD cardiac toxicity in the adult zebrafish heart. Journal of proteome research. 12, 3093-103.

Zhang T, Wang X, Shinn A, Jin J, Chan WK, 2010. Beta tubulin affects the aryl hydrocarbon receptor function via an Arnt-mediated mechanism. Biochem Pharmacol. 79, 1125-33.

Zhang X, Smits AH, van Tilburg G,B.A., Ovaa H, Huber W, Vermeulen M, 2018. Proteome-wide identification of ubiquitin interactions using UbIA-MS. Nature protocols. 13, 530.

Zhang Y, Huang L, Wang C, Gao D, Zuo Z, 2013. Phenanthrene exposure produces cardiac defects during embryo development of zebrafish (*Danio rerio*) through activation of MMP-9. Chemosphere. 93, 1168-75.

Zhang Y, Huang L, Zuo Z, Chen Y, Wang C, 2013. Phenanthrene exposure causes cardiac arrhythmia in embryonic zebrafish via perturbing calcium handling. Aquatic Toxicology. 142-143, 26-32.

Zhang Y, Wang C, Huang L, Chen R, Chen Y, Zuo Z, 2012. Low-level pyrene exposure causes cardiac toxicity in zebrafish (*Danio rerio*) embryos. Aquatic toxicology. 114, 119-24.

FIGURE AND TABLE CAPTIONS

Fig. 1. (A) Boxplots of the concentrations of pyrene measured in water by SFS after 1, 3, 7, 10 or 14 days of exposure (N = 3) or in tanks without fish (N = 14). **(B)** Average fluorescence spectrums for pyrene in the exposure water after 1, 3, 7, 10 or 14 days (N = 3), and in tanks without fish (N = 14).

Fig. 2. Heatmap displaying the proteins that were found to be differentially expressed in the heart of rainbow trout larvae, compared to the control group (DMSO) and after 7 days of exposure to either retene (RET, 32 $\mu g.L^{-1}$), pyrene (PYR, 32 $\mu g.L^{-1}$) or phenanthrene (PHE, 100 $\mu g.L^{-1}$). Proteins are displayed in rows and grouped according to similarities between treatments

961 by *k*-means clustering. Fold changes compared to the control group are expressed as log_2 values
962 and the color scale indicates the intensity. The proteins displayed in the present figure were
963 identified using the *O. mykiss* RefSeq database. N = 4 replicates per treatment and protein. *
964 indicates a significant difference compared to the control group.

965 **Fig. 3.** Heatmap displaying the proteins that were found to be differentially expressed in the
966 heart of rainbow trout larvae, compared to the control group (DMSO) and after 14 days of
967 exposure to either retene (RET, 32 $\mu g.L^{-1}$), pyrene (PYR, 32 $\mu g.L^{-1}$) or phenanthrene (PHE, 100
968 $\mu g.L^{-1}$). Proteins are displayed in rows and grouped according to similarities between treatments
969 by *k*-means clustering. Fold changes compared to the control group are expressed as log_2 values
970 and the color scale indicates the intensity. The proteins displayed in the present figure were
971 identified using the *O. mykiss* RefSeq database. N = 4 replicates per treatment and protein. *
972 indicates a significant difference compared to the control group.

973 **Fig. 4.** Bar plot showing the proteins identified exclusively by using the *S. salar* RefSeq database
974 and that were differentially expressed compared to the control group (DMSO) after 14 days of
975 exposure to either retene (RET, 32 $\mu g.L^{-1}$), pyrene (PYR, 32 $\mu g.L^{-1}$) or phenanthrene (PHE, 100
976 $\mu g.L^{-1}$). Fold changes compared to the control group are expressed as log_2 values and the error
977 bars represents the 95% confidence intervals. N = 4 replicates per treatment and protein. *
978 indicates a significant difference compared to the control group. [1] Full name: SWI/SNF-related
979 matrix-associated actin-dependent regulator of chromatin subfamily D member 3-like isoform
980 X6.

981 **Fig. 5.** Volcano plots of the metabolites identified in the heart of rainbow trout larvae after 14
982 days of exposure to either retene (RET, 32 $\mu g.L^{-1}$), pyrene (PYR, 32 $\mu g.L^{-1}$) or phenanthrene
983 (PHE, 100 $\mu g.L^{-1}$). Fold changes (x-axis) are expressed as log_2 values compared to the control

group (DMSO). The y-axis displays the -$\log_{10}$ adjusted *p*-values. The metabolites that were differentially expressed compared to the control group are featured in bold font and dark dots. Greyed dots represent the metabolites that were not significantly different compared to controls. N = 4 replicates per treatment and metabolite.

Table 1. Pathway (KEGG) enrichment analysis output from the cardiac tissue of rainbow trout larvae exposed to retene (RET, 32 µg.L^{-1}), pyrene (PYR, 32 µg.L^{-1}) or phenanthrene (PHE, 100 µg.L^{-1}) for either 7 or 14 days. The number of proteins or metabolites indicate the number of those that were detected and involved in the corresponding pathways, but not necessarily significantly differentially expressed in the datasets.

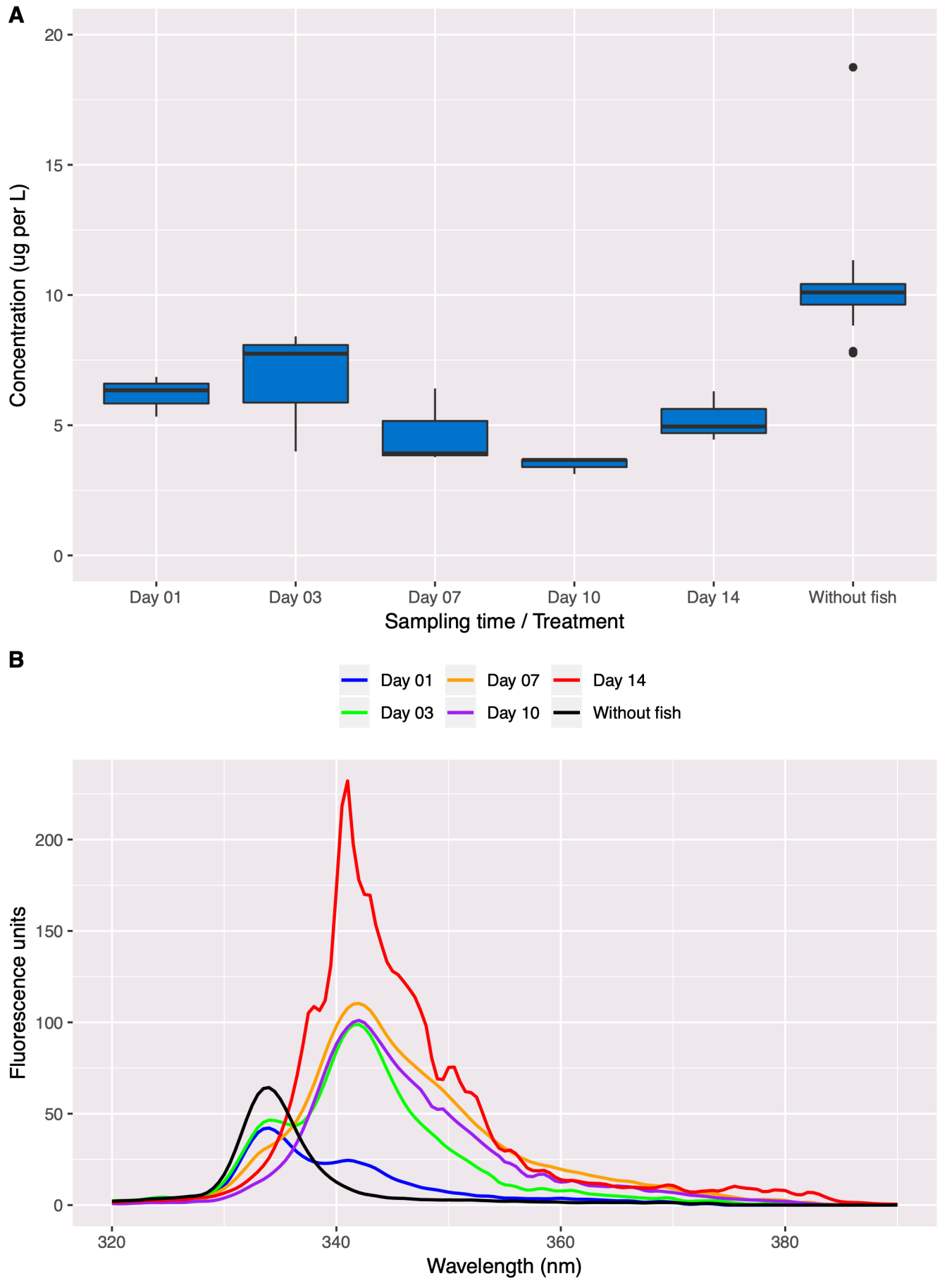
A
Concentration (ug per L)
20
15
10
5
0
Day 01
Day 03
Day 07
Day 10
Day 14
Without fish
Sampling time / Treatment
B
Day 01
Day 03
Day 07
Day 10
Day 14
Without fish
Fluorescence units
200
150
100
50
0
320
340
360
380
Wavelength (nm)

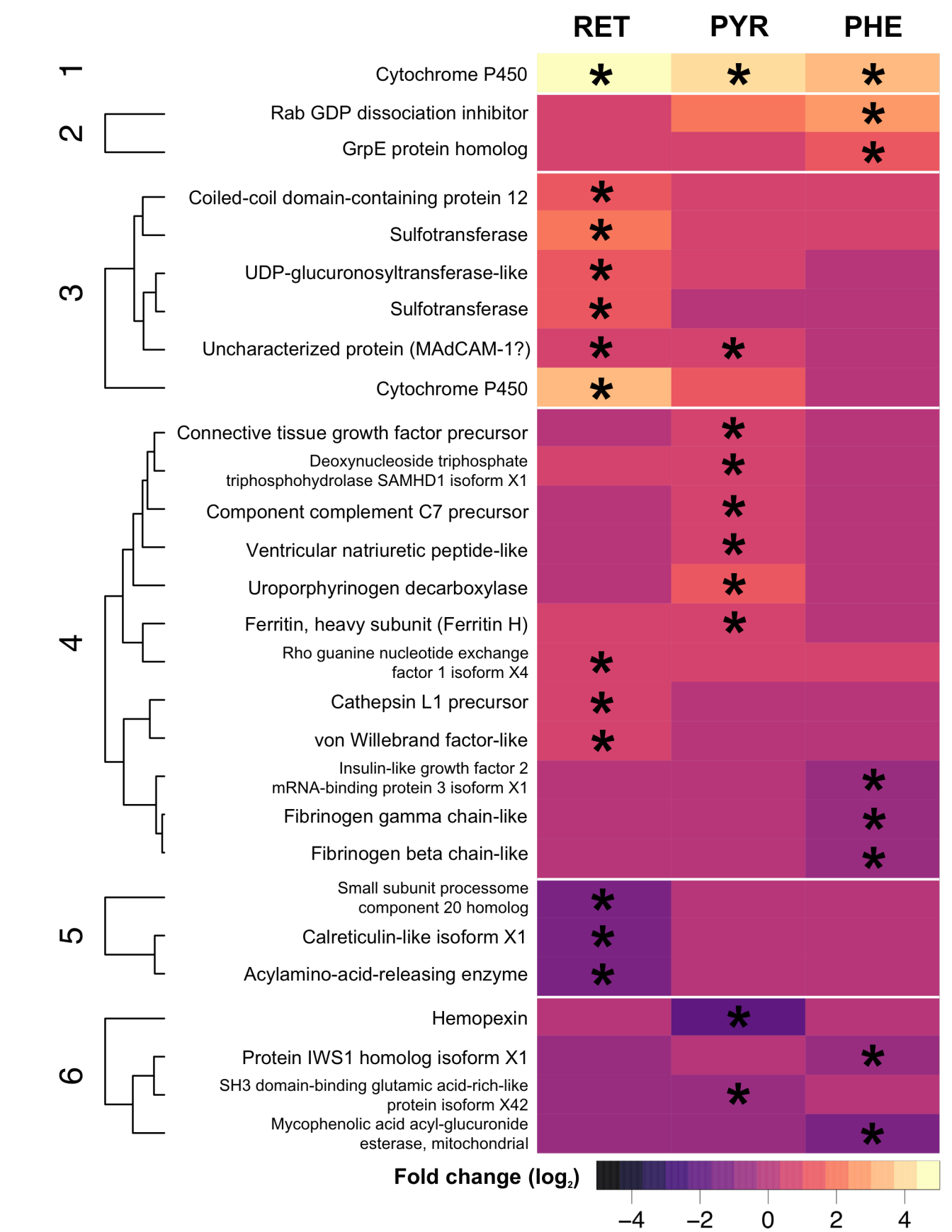
RET
PYR
PHE
1
2
3
4
5
6
Cytochrome P450
Rab GDP dissociation inhibitor
GrpE protein homolog
Coiled-coil domain-containing protein 12
Sulfotransferase
UDP-glucuronosyltransferase-like
Sulfotransferase
Uncharacterized protein (MAdCAM-1?)
Cytochrome P450
Connective tissue growth factor precursor
Deoxynucleoside triphosphate triphosphohydrolase SAMHD1 isoform X1
Component complement C7 precursor
Ventricular natriuretic peptide-like
Uroporphyrinogen decarboxylase
Ferritin, heavy subunit (Ferritin H)
Rho guanine nucleotide exchange factor 1 isoform X4
Cathepsin L1 precursor
von Willebrand factor-like
Insulin-like growth factor 2 mRNA-binding protein 3 isoform X1
Fibrinogen gamma chain-like
Fibrinogen beta chain-like
Small subunit processome component 20 homolog
Calreticulin-like isoform X1
Acylamino-acid-releasing enzyme
Hemopexin
Protein IWS1 homolog isoform X1
SH3 domain-binding glutamic acid-rich-like protein isoform X42
Mycophenolic acid acyl-glucuronide esterase, mitochondrial
Fold change (log2)
−4
−2
0
2
4

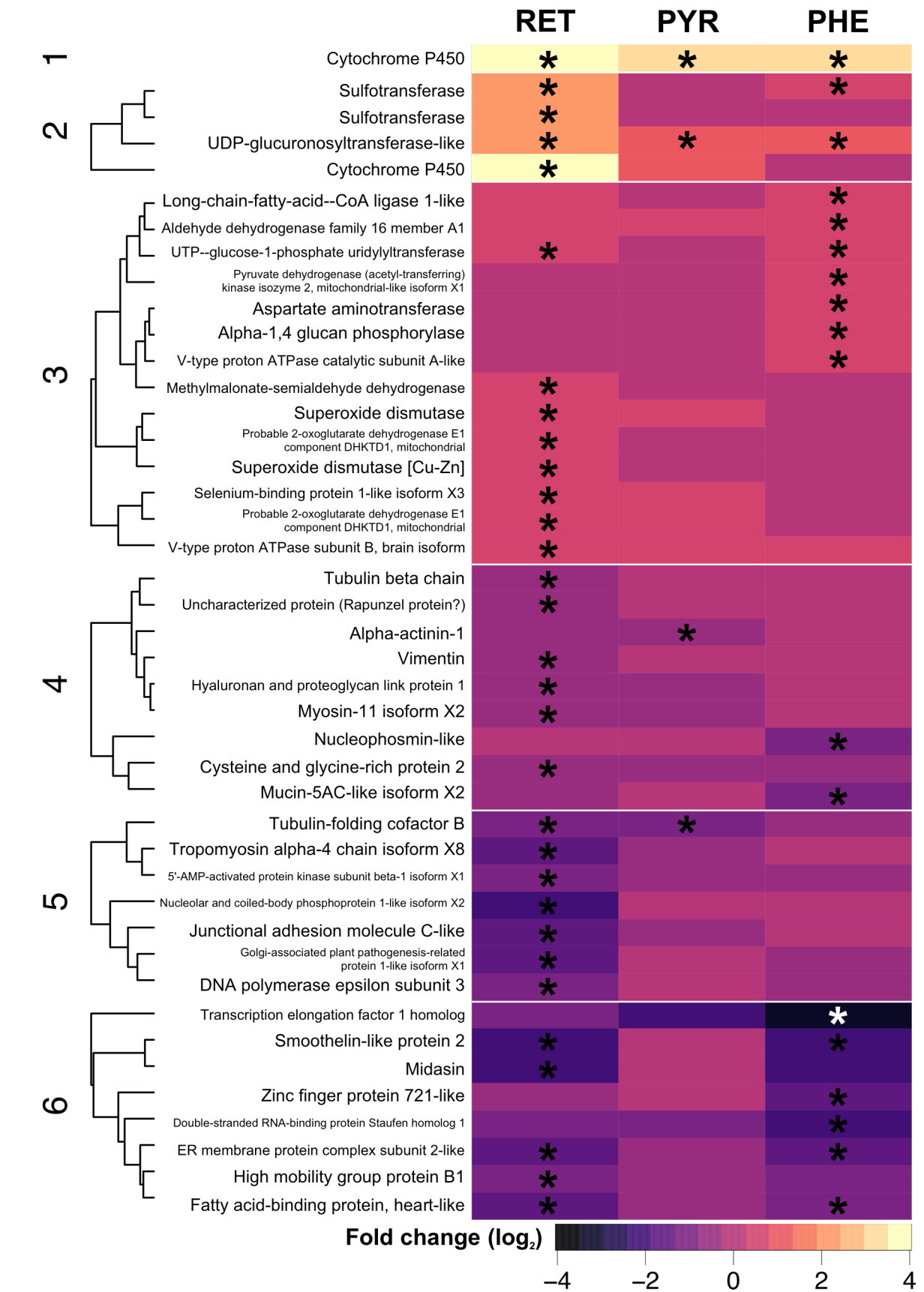
RET
PYR
PHE
1
2
3
4
5
6
Cytochrome P450
Sulfotransferase
Sulfotransferase
UDP-glucuronosyltransferase-like
Cytochrome P450
Long-chain-fatty-acid--CoA ligase 1-like
Aldehyde dehydrogenase family 16 member A1
UTP--glucose-1-phosphate uridylyltransferase
Pyruvate dehydrogenase (acetyl-transferring) kinase isozyme 2, mitochondrial-like isoform X1
Aspartate aminotransferase
Alpha-1,4 glucan phosphorylase
V-type proton ATPase catalytic subunit A-like
Methylmalonate-semialdehyde dehydrogenase
Superoxide dismutase
Probable 2-oxoglutarate dehydrogenase E1 component DHKTD1, mitochondrial
Superoxide dismutase [Cu-Zn]
Selenium-binding protein 1-like isoform X3
Probable 2-oxoglutarate dehydrogenase E1 component DHKTD1, mitochondrial
V-type proton ATPase subunit B, brain isoform
Tubulin beta chain
Uncharacterized protein (Rapunzel protein?)
Alpha-actinin-1
Vimentin
Hyaluronan and proteoglycan link protein 1
Myosin-11 isoform X2
Nucleophosmin-like
Cysteine and glycine-rich protein 2
Mucin-5AC-like isoform X2
Tubulin-folding cofactor B
Tropomyosin alpha-4 chain isoform X8
5'-AMP-activated protein kinase subunit beta-1 isoform X1
Nucleolar and coiled-body phosphoprotein 1-like isoform X2
Junctional adhesion molecule C-like
Golgi-associated plant pathogenesis-related protein 1-like isoform X1
DNA polymerase epsilon subunit 3
Transcription elongation factor 1 homolog
Smoothelin-like protein 2
Midasin
Zinc finger protein 721-like
Double-stranded RNA-binding protein Staufen homolog 1
ER membrane protein complex subunit 2-like
High mobility group protein B1
Fatty acid-binding protein, heart-like
Fold change (log2)
−4
−2
0
2
4

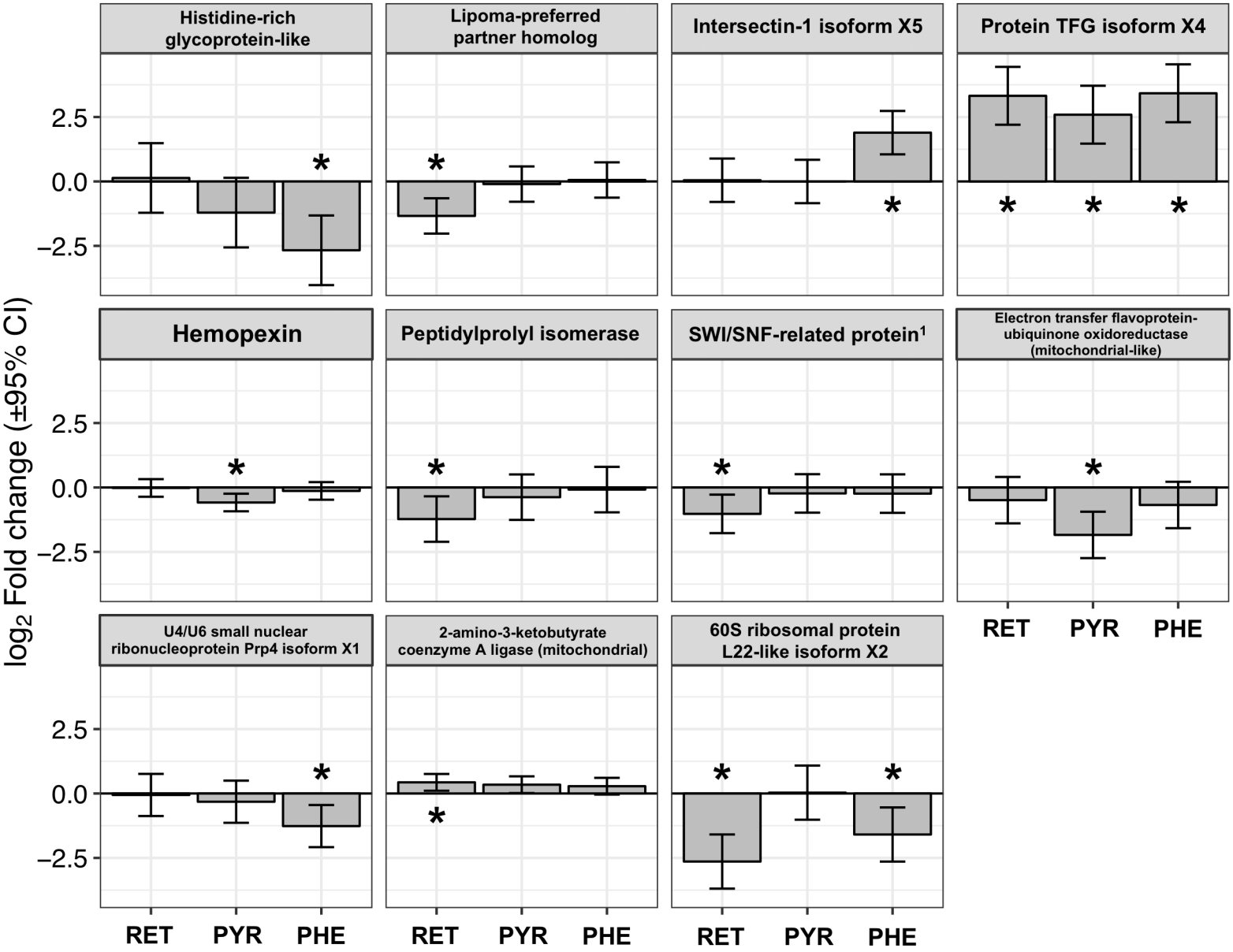
Histidine-rich glycoprotein-like
Lipoma-preferred partner homolog
Intersectin-1 isoform X5
Protein TFG isoform X4
Hemopexin
Peptidylprolyl isomerase
SWI/SNF-related protein[1]
Electron transfer flavoprotein-ubiquinone oxidoreductase (mitochondrial-like)
U4/U6 small nuclear ribonucleoprotein Prp4 isoform X1
2-amino-3-ketobutyrate coenzyme A ligase (mitochondrial)
60S ribosomal protein L22-like isoform X2
log2 Fold change (±95% CI)
2.5
0.0
−2.5
RET
PYR
PHE

Retene vs DMSO

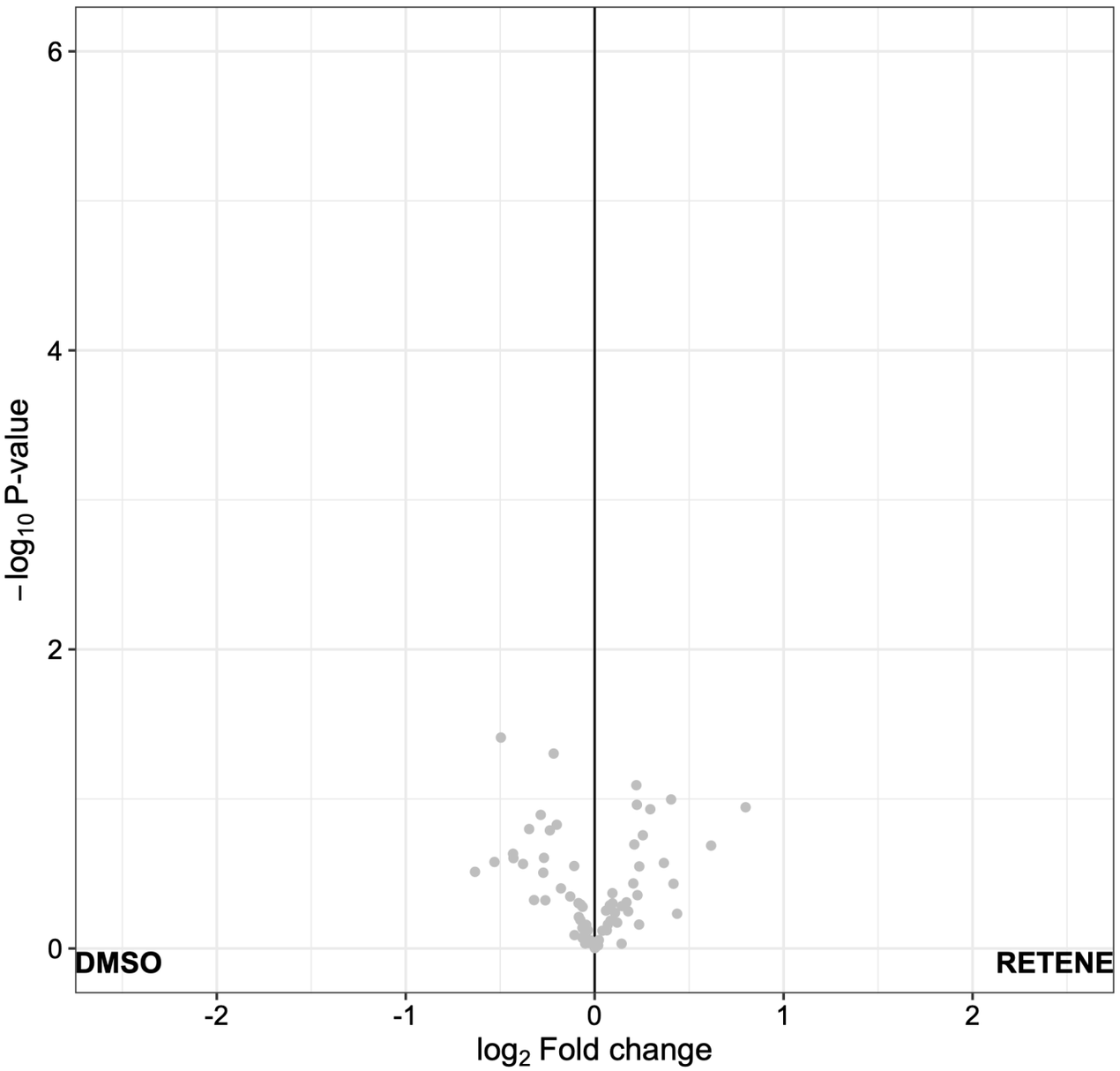

Phenanthrene vs DMSO

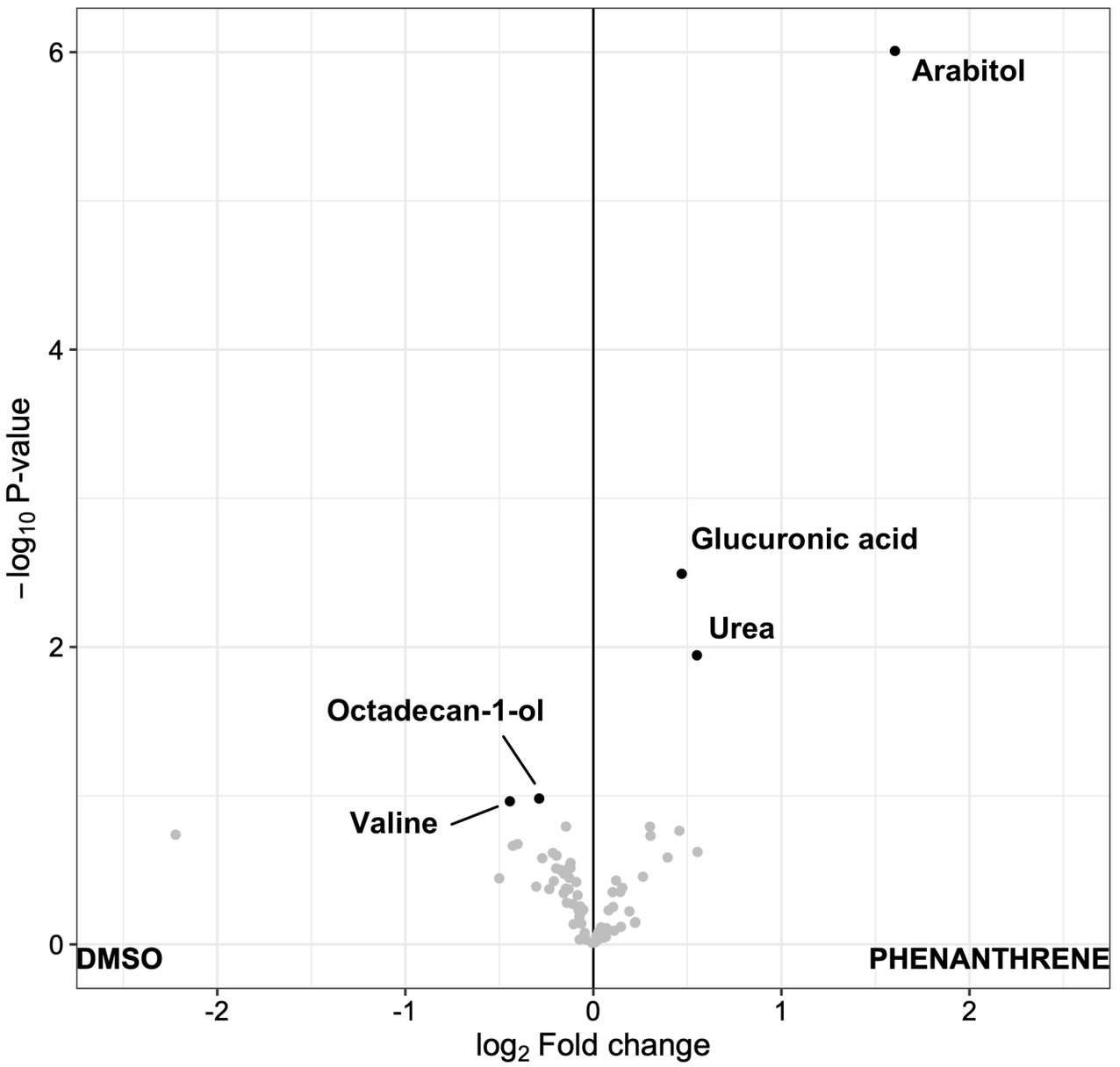

Pyrene vs DMSO

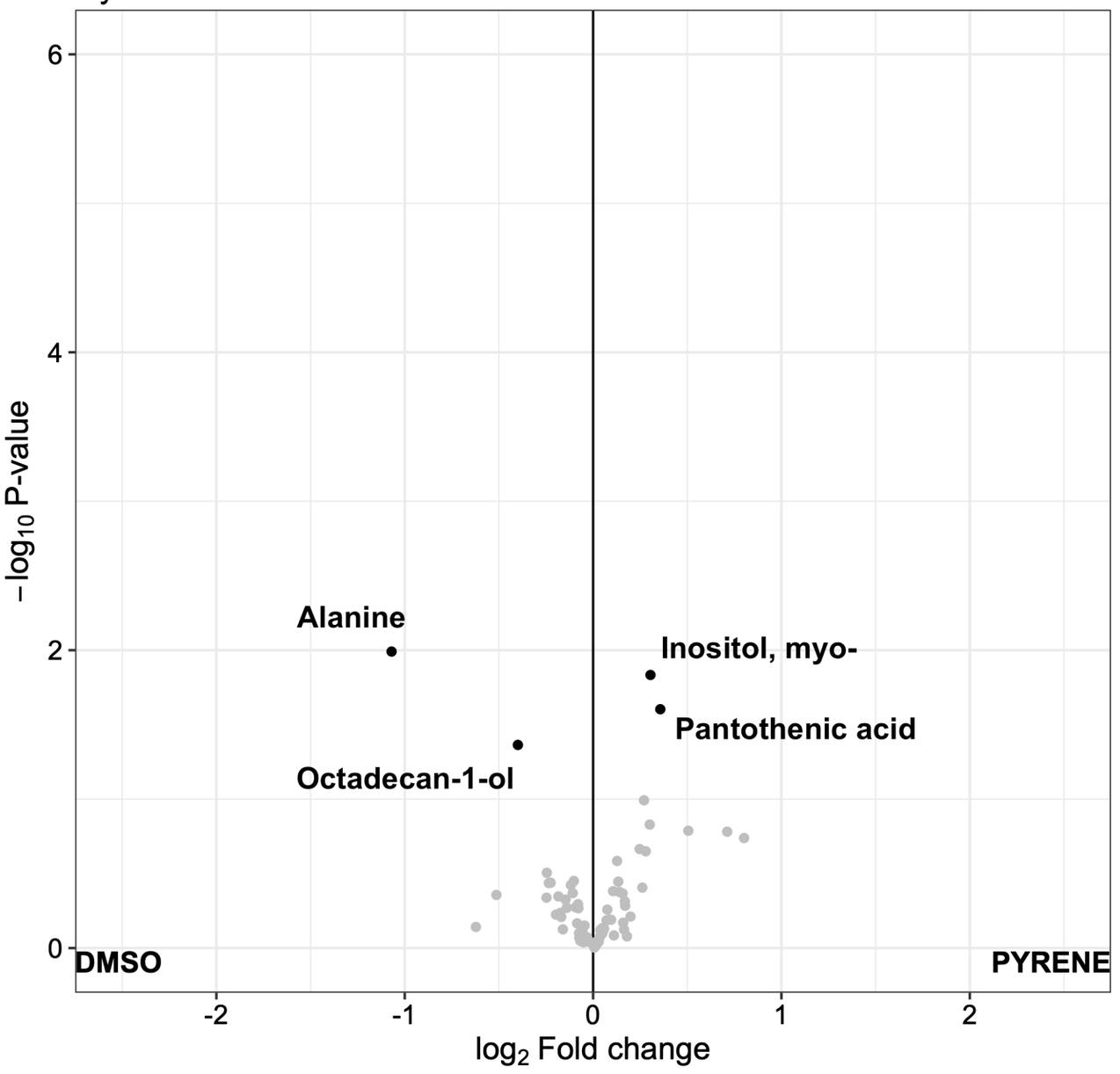

Sampling point (days)	Compound(s)	KEGG pathway	Pathway name	Proteins	Metabolites	*p* -value	Main proteins or metabolites involved
7	RET	dre00053	Ascorbate and aldarate metabolism	6	NA	$p \leq 0.05$	UDP-glucuronosyltransferase and UDP-glucose 6-dehydrogenase (NS[1])
		dre00982	Drug metabolism - cytochrome P450	8	NA	$p \leq 0.05$	UDP-glucuronosyltransferase
		dre00983	Drug metabolism - other enzymes	5	NA	$p \leq 0.05$	UDP-glucuronosyltransferase
		dre00040	Pentose and glucuronate interconversions	4	NA	$p \leq 0.05$	UDP-glucuronosyltransferase
		dre04145	Phagosome	28	NA	$p \leq 0.05$	Cathepsin and calcireticulin
		dre04270	Vascular smooth muscle contraction	14	NA	$p = 0.07$	See supplementary file 2A
	RET & PYR	dre00860	Porphyrin and chlorophyll metabolism	9	NA	$p \leq 0.05$	See supplementary file 2B
	RET, PYR & PHE	dre00980	Metabolism of xenobiotics by cytochrome P450	11	NA	$p \leq 0.05$	Cytochrome P450 and UDP-glucuronosyltransferase
		dre00830	Retinol metabolism	3	NA	$p \leq 0.05$	Cytochrome P450 and UDP-glucuronosyltransferase
		dre00140	Steroid hormone biosynthesis	4	NA	$p \leq 0.05$	Cytochrome P450 and UDP-glucuronosyltransferase
	PYR	dre04371	Apelin signaling pathway	20	NA	$p = 0.08$	See supplementary file 2C
		dre04216	Ferroptosis	10	NA	$p \leq 0.05$	See supplementary file 2D
14	RET	dre03410	Base excision repair	8	0	$p \leq 0.05$	See supplementary file 3A
		dre04068	FoxO signaling pathway	13	2	$p \leq 0.05$	See supplementary file 3B
		dre00562	Inositol phosphate metabolism	3	1	$p \leq 0.05$	Methylmalonate-semialdehyde dehydrogenase
		dre04146	Peroxisome	14	0	$p \leq 0.05$	Superoxide dismutase
		dre04530	Tight junction	46	0	$p \leq 0.05$	See supplementary file 3C
	RET and PHE	dre00040	Pentose and glucuronate interconversions	4	2	$p \leq 0.05$	UDP-glucuronosyltransferase, UTP--glucose-1-phosphate uridylyltransferase, UDP-glucose 6-dehydrogenase (NS[1]) and arabitol (PHE)
		dre00500	Starch and sucrose metabolism	8	2	$p \leq 0.05$	UTP--glucose-1-phosphate uridylyltransferase, glucose (RET, NS[1]), hexokinase (RET, NS[1]) and alpha-1,4 glucan phosphorylase (PHE)
	RET, PYR & PHE	dre00980	Metabolism of xenobiotics by cytochrome P450	11	0	$p \leq 0.05$	Cytochrome P450 and UDP-glucuronosyltransferase
		dre00830	Retinol metabolism	3	0	$p \leq 0.05$	Cytochrome P450 and UDP-glucuronosyltransferase
		dre00140	Steroid hormone biosynthesis	3	1	$p \leq 0.05$	Cytochrome P450 and UDP-glucuronosyltransferase
	PYR	dre04520	Adherens junction	18	0	$p = 0.06$	Alpha-actinin-1 and catenin delta-1 (NS[1])
		dre00982	Drug metabolism - cytochrome P450	9	0	$p \leq 0.05$	UDP-glucuronosyltransferase
		dre00983	Drug metabolism - other enzymes	5	1	$p \leq 0.05$	UDP-glucuronosyltransferase
	PYR & PHE	dre00380	Tryptophan metabolism	14	0	$p \leq 0.05$	See supplementary file 3D
	PHE	dre00053	Ascorbate and aldarate metabolism	6	2	$p \leq 0.05$	UDP-glucuronosyltransferase and aldehyde dehydrogenase
		dre00071	Fatty acid degradation	21	0	$p \leq 0.05$	Long-chain-fatty-acid--CoA ligase 1 and aldehyde dehydrogenase
		dre00360	Phenylalanine metabolism	3	1	$p \leq 0.05$	See supplementary file 3E
		dre00400	Phenylalanine, tyrosine and tryptophan biosynthesis	2	1	$p \leq 0.05$	Aspartate aminotransferase and phenylalanine

[1] Not significant.